Dissertation

submitted to the

Combined Faculties for the Natural Sciences and for Mathematics

of the Ruperto-Carola University of Heidelberg, Germany

for the degree of

Doctor of Natural Sciences

By

MS., Ravindra Peravali

Born in: Tirupati, India

Oral Examination date: January 26, 2018

Morphometric and Quantitative Behavioral Analysis of Inbred Medaka Lines

Referees

Prof. Dr. Joachim Wittbrodt

Prof. Dr. Nicholas Simon Foulkes

Dedicated to:

My parents

My wife and son

My teachers past and present

Declaration according to §8 (3) b) and c) of the doctoral degree regulations:

b) I hereby declare that I have written the submitted dissertation myself and in the process have used no other sources of materials than those expressly indicated.

c) I hereby declare that I have not applied to be examined at any other institution, nor have I used the dissertation in this or any other form at any other institution as an examination paper, nor submitted it to any other faculty as a dissertation.

Stutensee, November 17, 2018

Ravindra Peravali.

Parts of this thesis were published

- Herder, C., Swiercz, J. M., Müller, C., Peravali, R., Quiring, R., Offermanns, S., Wittbrodt, J. and Loosli, F. *ArhGEF18 regulates RhoA-Rock2 signaling to maintain neuro-epithelial apico-basal polarity and proliferation.* Development 140(13). May 2013.
- Spivakov, M., Auer, T. O., Peravali, R., Dunham, I., Dolle, D., Fujiyama, A., Toyoda, A., Aizu, T., Minakuchi, Y., Loosli, F., Naruse, K., Birney, E. and Wittbrodt, J. *Genomic and phenomic characterization of a wild Medaka population: Towards the establishment of an isogenic population genetic resource in fish.* G3-Gene Genomes Genetics 4(3). Jan. 2014.
- Sinn, R., Peravali, R., Heermann, S. and Wittbrodt, J. *Differential responsiveness of distinct retinal domains to Atoh7.* Mechanisms of Development. 133. Aug. 2014.

Parts of thesis are being prepared for publication

Authors: Peravali, R., Trivedi, C., Trost, N., Bollmann, J. and Wittbrodt, J.

Working Title: Let's prey: How Medaka reveals interspecific variability in prey capture behavior in Teleosts.

Acknowledgements

This work would not have been possible without the cooperation and goodwill of many people.

Firstly, I sincerely thank Prof. Dr. Joachim Wittbrodt who was not just my supervisor but an excellent guide and a strong pillar of support in times of need. I thank him for introducing me to Medaka and for allowing me to experiment freely with the different aspects of this wonderful model organism. A special thanks to the Wittbrodt Group meetings which were intense, challenging and intellectually satisfying.

Dr. Johann Bollmann and Dr. Chintan Trivedi have been an invaluable part of this work. The prey capture work in this thesis is a reflection of this fantastic collaboration. I would like to thank Chintan for sharing his experiences from the zebrafish world and for the many discussions we have had. Dr. Bollmann was instrumental in my understanding of how to quantify behavioral parameters and for showing me the right way to do things.

I thank Prof. Nicholas Foulkes and Dr. Ralf Mikut for their suggestions and support. I also thank Dr. Jan-Felix Evers for agreeing to be a part of my examination committee.

The support that I have received from the Institute of Toxicology and Genetics and the Karlsruhe Institute of Technology (KIT) has been immense. I specially thank Prof. Dr. Uwe Strähle, Dr. Sandra Schneider and the entire administrative staff for their help. I thank Dr. Larissa Kaufmann for helping me in times of need. A special thanks to the La

rge Scale Data Facility at the KIT for generously offering IT services. I also thank Dr. Urban Liebel who allowed me to pursue my scientific interests.

This work would not have been possible without the active support and help of the Medaka facility at the KIT. I thank Dr. Felix Loosli, Nadeshda Wolf, Natalja Kusminski and Nadine Eschen. I thank Dr. Thomas Auer with whom I started the phenotypic characterization of Medaka. I would also like to thank Eduard Gursky who assisted in the development of the robotic imaging platform.

My wife, Nagashree (Deepulu!) Peravali, has been my principle motivator. She has had to go through a lot in the last few years and I express my heartfelt thanks. My son Aditya Peravali has been understanding and a fun companion during stressful times. My parents, Dr. Hanuman Prasad and Mrs. Lalitha Prasad, are the two influential people in my life. I thank my family for everything and this work is a reflection of your love and understanding.

Table of Contents

Summary

With advances in genotyping and cost-effective sequencing technologies, Genome-wide association studies (GWAS) have emerged as approaches to study the genetics of natural variation. GWAS are particularly useful when inbred lines are available (as once they are genotyped, these lines can be phenotyped multiple times) and also with the availability of automated image acquisition and analysis systems for rapid phenotyping. The objective of this thesis is to identify a variety of phenotypic traits from the inbred lines of the teleost fish Medaka (*Oryzias latipes*) which will then assist in the investigation of the genetic basis for such a variety. Medaka is chosen as the model organism because of the presence of still free living wild populations in Japan and East Asia and for the ability to generate new inbred strains from these wild fish. Moreover, Quantitative Trait Loci (QTL) analysis done so far on craniofacial traits in adult Medaka shows that a substantial genetic component underlies the variance seen between two inbred strains. In this study different southern and northern Japanese Medaka hatchlings at 10 days post fertilization (dpf) and 20 dpf were characterized. The focus is on the two elements that essentially define an organism: morphology and behavior. Gross morphological features were extracted and quantified using custom developed algorithms. In addition, behavioral patterns of the different inbred lines are studied since behavior provides a link and a perspective of how an organism relates to its environment. Specifically, locomotion, feeding, and prey capture behavior were analyzed and quantified. To our knowledge, this is the first characterization of prey capture behavior in Medaka. This behavior reveals interesting prey capture strategies and a comparison with a related teleost fish, the zebrafish, suggests that prey capture is not necessarily conserved. This combination of morphometric and behavioral features provides a large phenotype parameter

set that will be used as a basis for genotyping to study the degree of polymorphism and to eventually establish a phenotype-genotype map for the inbred lines.

Zusammenfassung

Genom – weite Assoziationsstudien (GWAS) werden dazu eingesetzt, um natürliche Genotyp- Variationen zu untersuchen. Die Vorteile dabei liegen beim Genotypisieren und kostengünstigen Technologien für die Sequenzierung.

GWAS sind besonders nützlich, wenn Inzucht-Linien vorliegen (sobald diese genotypisiert sind, können diese Linien vielfach phänotypisiert werden). Diese GWAS können mit automatisierten Bildgebungsverfahren und Analysesystemen zur Phänotypisierung kombiniert werden. Ziel dieser Arbeit ist es eine große Vielfalt an phänotypischen Merkmalen von Inzuchtlinien des Knochenfisches: Medaka (*Oryzias latipes*) zu identifizieren. Diese sollen dabei helfen, die genetischen Grundlagen, die diese Vielfalt begründen, zu bestimmen. Medaka wird als Modelorganismus gewählt, da es immer noch Wildtyp -Linien in Japan und Ost-Asien gibt, aus denen neue Inzucht-Linien gewonnen werden können. Zusätzlich zeigen quantitative Merkmals- Analysen (Quantitative Trait Loci (QTL)) der Gesichtsknochen des adulten Medaka, dass die Variabilität zwischen zwei Inzucht Fischlinien von bedeutenden genetischen Komponenten abhängt. In dieser Arbeit werden verschiedene Süd- und Nord-japanische Linien 10 und 20 Tage nach Befruchtung charakterisiert. Der Fokus liegt dabei auf der Morphologie und dem Verhalten. Dies sind zwei Elemente, die einen Organismus definieren. Morphologische Merkmale werden durch selbst entwickelte Algorithmen extrahiert und quantifiziert. Zusätzlich werden Verhaltensmerkmale der verschiedenen Inzuchtlinien beobachtet, da Verhalten zeigt, in wie fern ein Organismus mit seiner Umwelt verbunden ist. Besonders Fortbewegung, Fressverhalten und Beuteverhalten werden analysiert und quantifiziert. Das ist das erste Mal, dass in Medaka das Beuteverhalten charakterisiert wird. Es wird demonstriert, dass es interessante Beutestrategien gibt. Ein Vergleich mit verwandten Knochenfischen zeigt, dass Beuteverhalten

nicht zwingend in der Evolution konserviert ist. Die Kombination von morphometrischen Untersuchungen und Verhaltensstudien erlaubt es, viele phänotypische Parameter zu untersuchen, um damit eine Grundlage für weitere Genotypisierungen zu schaffen. Damit soll der Grad von Polymorphismus bestimmt werden und eine Phänotyp-Genotyp-Karte für die Inzucht-Linien aufgebaut werden.

Introduction

Two elements that define and describe an organism are its morphology and behavior. Every population displays a variety in morphological and behavioral phenotypes. This polymorphism could be the result of genetic diversity, environmental cues or a combination of both. It is of fundamental biological interest to understand this phenotypic variation, to characterize this variation and be able to establish a relationship between the observed phenotypes and the underlying genotype. This genotype-phenotype (G-P) map has the potential to address individual risk factors and in establishing a new paradigm directed towards personalized medicine.

Phenomics

Since the realization of the Human Genome Project, there has been an increased interest in large-scale phenotyping as a natural complement to genome sequencing. This phenomic data is of vital importance in understanding the effects of genetic variation, pleiotropy and will contribute to deciphering the complex phenomena of health, disease and evolutionary viability. The acquisition of high-dimensional phenotypic data at the whole-organism level is currently defined as “phenomics” (Houle, Govindaraju, & Omholt, 2010; Soule, 1967). The importance of phenomics lies in its ability to allow for the identification of causal links between genotypes, environmental factors and phenotypes and thereby in establishing the genotype-environment-phenotype (G-E-P) map. The concept of the G-E-P map is described in Figure 1 and is adapted from (Houle et al., 2010). Any individual of a population occupies a single point in the G-space. The interaction between this position, other members of the population and the environment gives rise to the internal phenotypic state. Internal phenotypes are typically cellular, tissue level

and physiological properties. The internal phenotypes influence the external phenotypes (morphology and behavior) which in turn shapes the environment that the individual inhabits. This creates a complex relationship between the genetics of the individual, the environment and the phenotypes providing the G-E-P map (Houle, 2010; Houle et al., 2010).

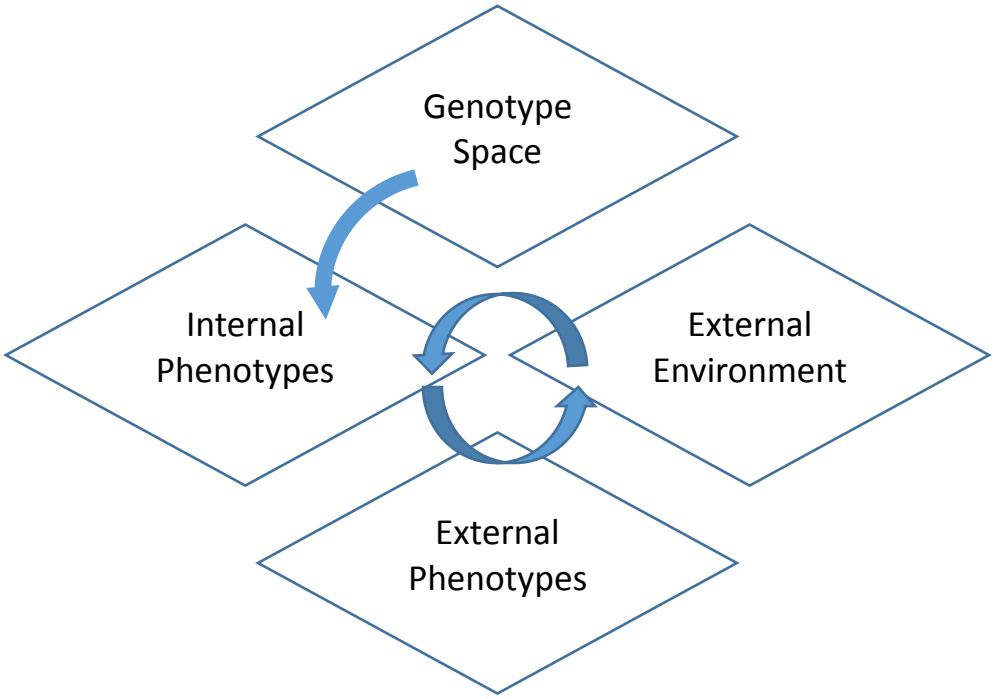

Figure 1 The Genotype-Environment-Phenotype (G-E-P) map describes the interaction between individual genotypes, the environment and the internal and external phenotypes

Table 1 shows some recent efforts in understanding this map in different species with emphasis on identifying phenotypes based on existing genetic variation (Bilder et al., 2009; Houle et al., 2010).

Species	Description	Phenotypes	Genotyping	Links
Plants	International Plant Phenotyping Network (IPPN)	Quantitative, high-throughput, non-invasive imaging of small model and crop plants; metabolomes		http://www.plantphenomics.com
Arabidopsis	Phenotyping and GWA studies on 191 inbred lines	107 quantitative phenotypes like flowering traits, life history, etc.	250,000 SNPs	http://walnut.usc.edu/2010/GWA
Drosophila	*Drosophila* Genome Reference Panel	Physiology, disease resistance, gene expression, behavior and morphology.	About 200 lines sequenced	http://flybase.org/static_pages/news/whitepapers/Drosophila_Genetic_Reference_Panel_Whitepaper.pdf
Mouse	The Mouse Phenome Database (MPD) phenotype information for common inbred lines	Wide variety of phenotypes including morphology, behavior, physiology, etc.	SNP typing of inbred lines	http://www.jax.org/phenome http://www.europhenome.org
Rat	National BioResource Project	109 qualitative and quantitative phenotypes	357 simple sequence length polymorphisms cover genomes	http://www.anim.med.kyoto-u.ac.jp/nbr
Dog	Canine Phenome Project	Heritable diseases, behavior	SNP typing of different breeds	http://www.caninephenome.org
Human	Consortium of Neuropsychiatric Phenomics; UK Biobank; Personal Genome Project	Brain imaging, behavior, physical measurements, cell lines, medical history	Birth-cohorts, case-control genotyping, genome sequencing	http://www.phenomics.ucla.edu http://www.ukbiobank.ac.uk http://www.personalgenomes.org

Table 1 Phenome projects focusing on characterization of phenotypes of existing genetic variation

Forward Genetic Screens

Given that the G-E-P map or the G-P map can be of significance in revealing risk factors and in the manifestation of specific traits in a population, the question is how to choose the best way to obtain this map. One of the most powerful tools to address this is forward genetic screening. In this method, individuals of a population differing in genotype are screened for phenotypes of interest. The genetic differences can be obtained either by sampling the natural population or by mutagenesis. The identified phenotypes can then be linked to the causative loci via mapping approaches like the Quantitative Trail Loci (QTL) mapping (Korte & Farlow, 2013). As opposed to qualitative traits (Mendelian) which have an "either-or" expression, quantitative traits (like height or weight) manifest as a result of both genetic and environmental effects. These traits may be discrete, like the number of digits on a limb, or may vary continuously across a population, like height or weight. A QTL is a genetic locus whose alleles are responsible for the variation (Abiola et al., 2003; Grisel, 2000). QTL mapping is a powerful tool that samples several regions across the genome that co-segregate with a trait of interest in either F2 populations or in Recombinant Inbred Line (RIL) families. However, this places a limitation on forward genetics with QTL mapping as it is useful only when there is a variation in a population for a given trait or when such differences can be generated via crosses. Furthermore, only allelic diversity among the F2 founders or within the RIL population can be assayed and the amount of recombination during the creation of the RIL population limits the mapping resolution. This approach is not suitable in species that are reproductively isolated (Abiola et al., 2003; Borevitz & Nordborg, 2003; Korte & Farlow, 2013; Pardo-Diaz, Salazar, & Jiggins, 2015).

Genome Wide Association Studies (GWAS)

In the recent years, a complementary approach to establish the G-P map has emerged to overcome some of the limitations of forward genetics. An association mapping approach, the Genome Wide Association Study builds on the most common genomic variation, the Single Nucleotide Polymorphism (SNP). A SNP is a variation in a single nucleotide at a specific position in the genome with the variation present to some appreciable degree in a population. GWAS make use of the historical recombination in wild populations and detect associations between SNPs and the trait of interest scored over a large number of individuals (Hunter, Wright, & Bomblies, 2013; Pardo-Diaz et al., 2015; Shimizu & Purugganan, 2005; Stinchcombe & Hoekstra, 2008). GWAS can be conducted to (Pardo-Diaz et al., 2015):

1. Identify causative/predictive factors for a given trait
2. Establish a genetic architecture of a trait - determine the number of loci that contribute to and the extent of contribution to the trait.

The ability to detect association between the SNP alleles and the trait depend on the Linkage Disequilibrium (LD) between the alleles and the surrounding SNPs. In order to understand LD better, suppose that in a population, p_A is the frequency of allele A at a locus and p_B is the frequency of allele B at another locus. Suppose also that p_{AB} is the frequency of the AB haplotype. Now, if the association between the alleles A and B is completely random and the occurrence of one does not influence the occurrence of the other, then the probability that both A and B occur together is the product $p_A p_B$. If, however, p_{AB} differs from the product $p_A p_B$ then the alleles are said to be in a linkage disequilibrium. The coefficient of linkage disequilibrium is given by

$$D_{AB} = p_{AB} - p_A p_B. \quad (1)$$

GWAS identify novel loci defined by the LD blocks (known as haplotype blocks) (Cox & Church, 2011; Manolio, 2010; Moffatt, Traherne, Abecasis, & Cookson, 2000; Pardo-Diaz et al., 2015; Slatkin, 2008; Spivakov et al., 2014).

One of the important requirements to conduct GWAS is an appropriate model organism. The extent to which GWAS can identify a true association between a SNP and a trait is dependent on the phenotypic variation within the population as explained by the SNP. This variance is determined by how two allelic variants differ in their phenotypic effects (the effect size) and the frequency of these variants in the population. Furthermore, an ideal model organism is one that can be potentially maintained as inbred lines so that it is possible to repeatedly phenotype these lines of genetically identical individuals while also significantly improving the mapping resolution (Cox & Church, 2011; Korte & Farlow, 2013; Stinchcombe & Hoekstra, 2008).

Medaka as a model organism

Fish constitute the largest class of vertebrates. While fish diverged from humans more than 400 million years ago, there are substantial similarities that justify the study of fish and their translational relevance (Postlethwait et al., 2000; Schartl, 2014). With minor differences at the biological organization level, there are very few differences at the molecular level (Postlethwait et al., 2000; Schartl, 2014). Furthermore, fish offer several unique advantages: fish models are usually small and their maintenance and breeding is large numbers is relatively easy and low cost. Secondly, they are amenable to genetic modifications including transgenesis and gene knock-out. Finally, they are an ideal model for high-throughput approaches.

The teleost fishes consisting of about 27 000 species are the largest and the most diverse group exhibiting a phenomenal variation in morphology, behavior and ecological adaptations. One of the reasons for this diversity is believed to be a whole genome duplication (WGD) event that occurred at the base of the teleost radiation as shown in Figure 2a (Furutani-Seiki & Wittbrodt, 2004; Ravi & Venkatesh, 2008; Takeda & Shimada, 2010).

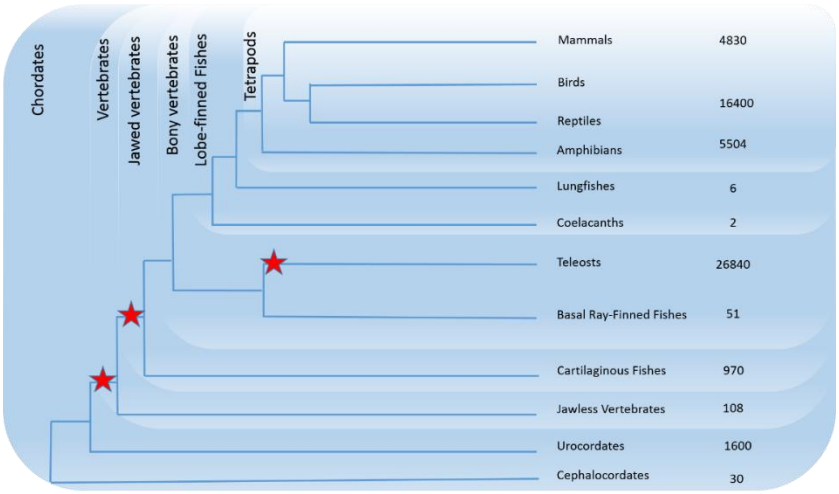

(a)

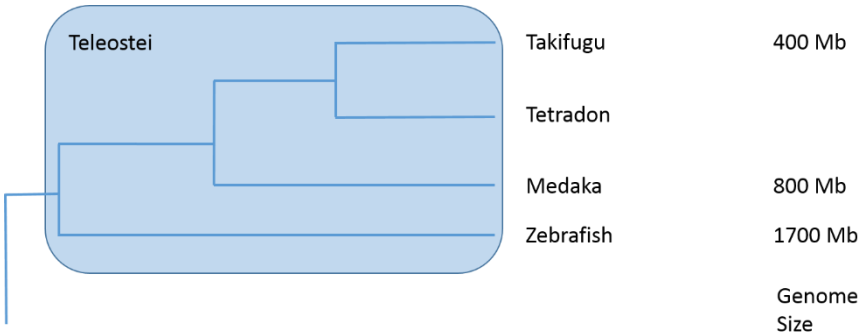

(b)

Figure 2 Phylogenetic tree of chordates. (a). Three major Whole Genome Duplication depicted by red stars. The topmost WGD event occurs in the teleost ancestor. (b). Teleost radiation showing the reduction in genome size.

Owing to the WGD, fish resulted in having two copies of many genes of which other vertebrates had only one. This manifests in altered gene expression or protein functions so that the complement of the gene expression patterns or protein functions of both fish paralogs are equivalent to the single vertebrate ortholog (Furutani-Seiki & Wittbrodt, 2004; Meyer & Schartl, 1999; Postlethwait et al., 2000; Ravi & Venkatesh, 2008; Schartl, 2014). This process termed subfunction partitioning has significant consequences in the study of the function of these genes. Furthermore, when such genes have multiple functions the fish model becomes extremely relevant because different phenotypes resulting from these genes can be studied separately (Force et al., 1999; Schartl, 2014). An example provided in (Schartl, 2014) suggests that if a gene in mouse that is responsible for early development and in an organic-specific function at adulthood is mutated, it becomes impossible to understand the organ-specific function of this gene. However, in fish both functions are partitioned between the duplicates making the study of both phenotypes possible.

In the recent decades, the zebrafish (*Danio rerio)* has emerged as an important and widely used model organism for studying development and disease (Jing & Zon, 2011; MacRae & Peterson, 2015; Santoriello & Zon, 2012; Zon & Peterson, 2005). The zebrafish offer several advantages like high fecundity, short developmental time, transparent embryos, ease of creating transgenic lines, etc. Zebrafish have been extensively used for mutagenesis screens (Amsterdam & Hopkins, 2006; Driever et al., 1996; Mullins, Hammerschmidt, Haffter, & Nusslein-Volhard, 1994) and chemical screens (Brady, Rennekamp, & Peterson, 2016; Kokel & Peterson, 2011; Peterson & Fishman, 2011). However, in order to be able to decipher general genetic principles and to understand conserved and species-specific genetic and molecular mechanisms, it is vital to study and

compare two related species (Furutani-Seiki & Wittbrodt, 2004). Due to the teleost lineages having evolved independently after the gene duplication event, it is possible that different fish species will show differences in the fate of the duplicated genes. Consequently, under the “complementarity argument”, comparing two divergent teleost species can be revealing and provide a better understanding of the evolution of genetic and molecular networks (Furutani-Seiki & Wittbrodt, 2004; Schartl, 2014). Additionally, certain disadvantages of the zebrafish, like the lack of consistent success in inbreeding, warrants the necessity of a related model organism that can overcome these disadvantages while bringing in potential advantages.

A related species (Figure 2b) sharing most of the advantages of the zebrafish, Medaka has a history of more than 100 years of genetic research. Medaka, *Oryzias latipes*, is a small egg-laying freshwater teleost fish primarily found in Japan, Korea, Taiwan and China (Takeda & Shimada, 2010; Wittbrodt, Shima, & Schartl, 2002) (Figure 3). It is closely related to members of the ray-finned fish like the pufferfish, stickleback and killifish. It is separated from zebrafish by about 150 million years of divergent evolution (Kirchmaier, Naruse, Wittbrodt, & Loosli, 2015; Shima & Mitani, 2004; Takeda & Shimada, 2010; Wittbrodt et al., 2002).

In Japan, Medaka are found in small rivers, creeks and rice paddies. The adults grow up to 4 cm in length and the females can lay between 10 – 30 eggs per day. Similar to the zebrafish, the embryo fertilization is external and the chorion and the embryos are transparent (Takeda & Shimada, 2010) (Figure 3c). The embryos usually hatch between 7 and 10 days post fertilization (dpf) and reach sexual maturity within 2.5 months.

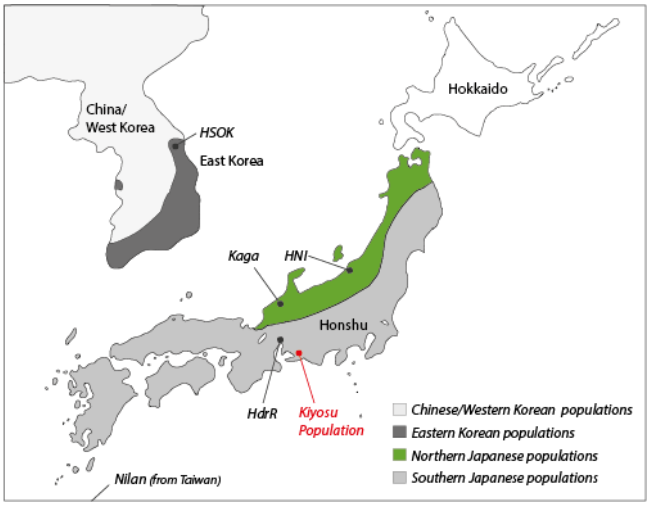

(a)

(b)

(c)

Figure 3 (a). Geographical distribution of Medaka. From (Spivakov et al., 2014). (b). Typical Medaka in an aquarium. (c). Transparent hatchling at 10 dpf.

In addition to these features, Medaka offers several advantages over zebrafish. Firstly, the size of the genome is half that of zebrafish at 800 Mb. Secondly, Medaka are highly polymorphic with high degree of genetic variation (Figure 3a shows the population distribution). This makes them an ideal model for studying population genomics, speciation and for GWAS. Finally, Medaka is a eurythermal fish. They can survive between 0 °C and 40 °C. This makes them ideal for microinjections, transplantation, etc. as the embryonic development can be slowed down using low temperatures (~ 4 °C) or even arrest cell cycle progression of blastomeres (Shima & Mitani, 2004; Takeda & Shimada, 2010; Wittbrodt et al., 2002). A requirement for a model organism to be used for research purposes is a detailed developmental staging. Figure 4a – 4d show the

staging series taken from (Iwamatsu, 2004). Further details can be obtained from (Iwamatsu, 2004; Shima & Mitani, 2004; Wittbrodt et al., 2002).

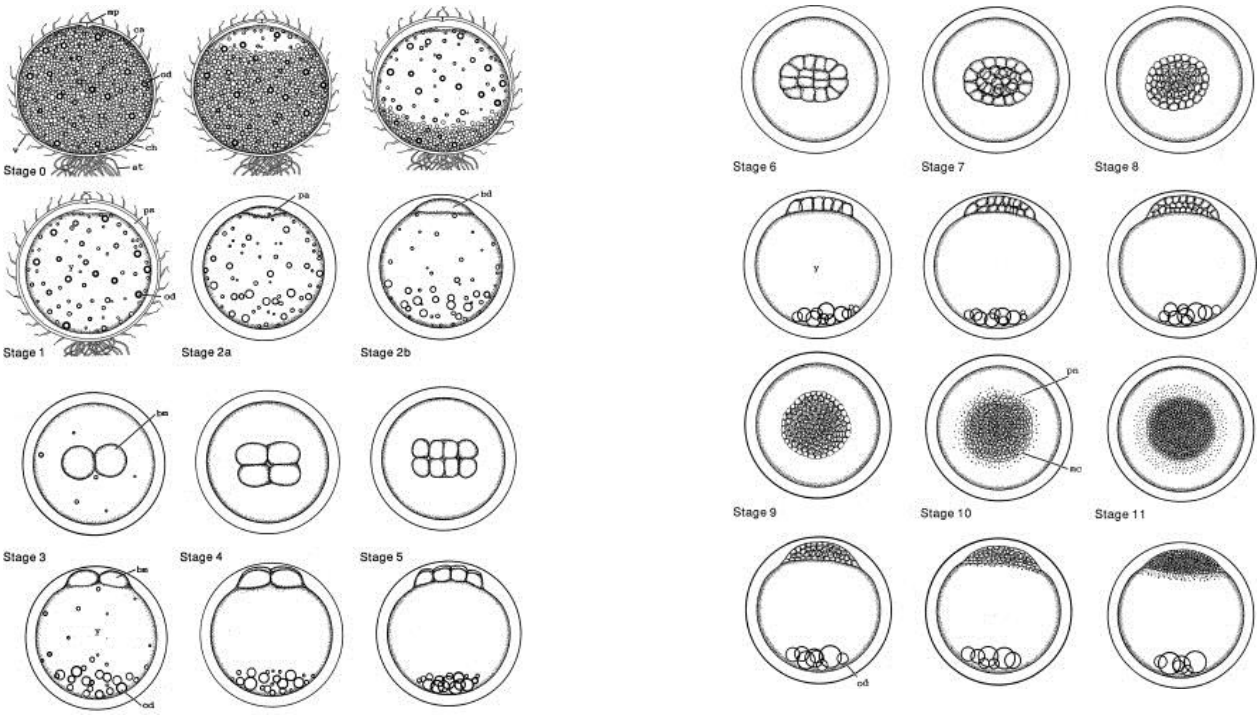

(a)

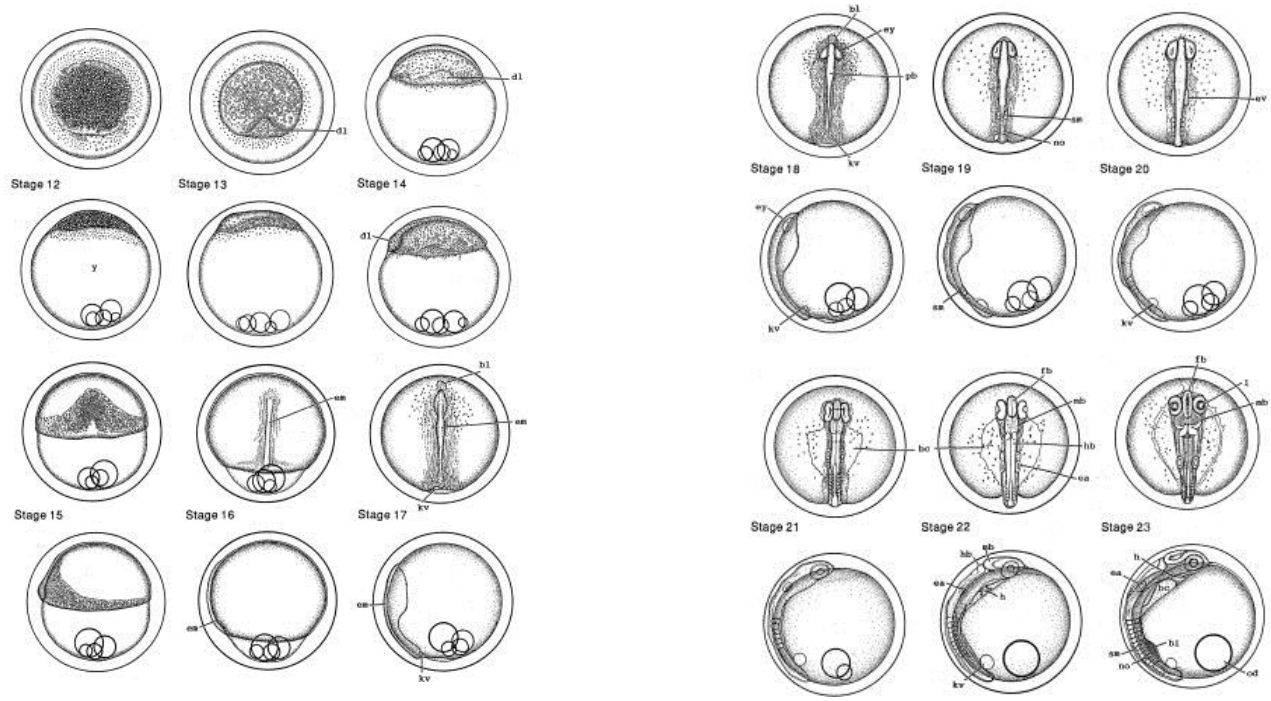

(b)

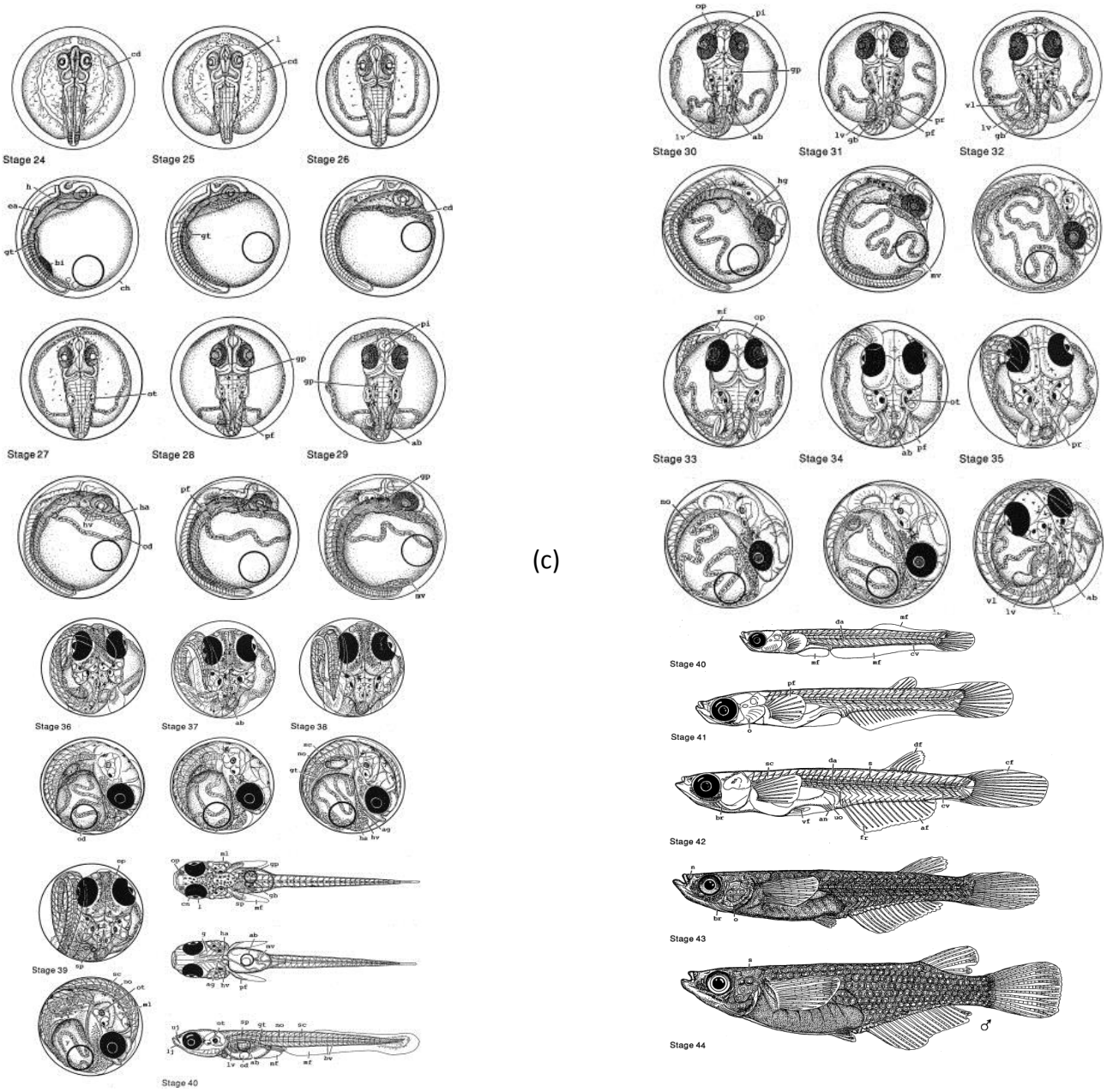

Figure 4 Stages of Medaka development. (a). Stage 0: Unfertilized eggs; Stage 1: Activated egg stage; Stage 2: Blastodisc stage; Stage 3 – 7: 2 cell to 32 cell stage; Stage 8 – 9: Early and late morula; Stage 10 – 11: Early and late blastula. (b). Stage 12 – 16: Pre-, mid- and late gastrula; Stage 17 – 18: Early and late neurula; Stage 19 – 23: 2 somite to 12 somite stages. (c). Stage 24 – 35: 16 to 35 somite stage; Stage 31: Gill blood vessel; Stage32: Somite completion; Stage 33: Completion of notochord vacuolization; Stage 34: Pectoral fin blood circulation; Stage 35: Start of formation of visceral blood vessels. (d). Stage 36: Heart development; Stage 37: Formation of pericardial cavity; Stage 38: Spleen development; Stage 39: Hatching (around 9 days); Stage 40 – 44: From first fry stage with ~4.5 mm total length to stage with total length greater than 25 mm. From (Iwamatsu, 2004).

to address fundamental and related issues (Flint & Mackay, 2009): (1) Estimate interspecific differences in genetic architecture. (2) Estimate variation of genetic architecture between phenotypes. (3) Identify if same genes are responsible for same phenotypes across species. There are two classical approaches to creating defined genetic reference panels of inbred lines (Bailey, 1971; Flint & Mackay, 2009; Spivakov et al., 2014). The first approach is to establish the panel via crossing of a few genetically distinct founders and following it up with a series of interbreeding steps that will then lead to an outcrossed population. This outcrossed population is then inbred to obtain recombinant inbred lines (RILs). The second approach is to use individuals from a wild population and inbreed them successively to give rise to near NILs. Both methods provide panels that have specific benefits (Bailey, 1971; Flint & Mackay, 2009; Spivakov et al., 2014). Firstly, since the same genotype can be reproduced several times from the panel, it offers a common resource to the research community. Secondly, nongenotypic variance can be overcome because of the possibility of making measurements from different individuals with the same genetic background. Lastly, the G-E-P interaction can be well studied by systematically varying the environment of different individuals with the same genotype. RILs provide a straightforward approach to characterizing the genetic background of a population while often being able to relate the phenotypes back to the founders. However, with this approach the mapping resolution is limited by the number of recombinations available in the panel and the panel diversity itself is limited by the diversity of the input founders. This poses a restriction on the ability to discover interesting traits. On the other hand, NILs have greater diversity and better recombination patterns which allows for the discovery of more traits and finer mapping resolution.

Over the last several decades, RILs and NILs have been used extensively. The yeast community has used such methods for genotype-phenotype mapping (Bloom, Ehrenreich, Loo, Lite, & Kruglyak, 2013; Liti et al., 2009) . In the plant research community a panel of 302 IBM maize strains (Fu et al., 2006; Sharopova et al., 2002) and the set of 107 strains in *Arabidopsis* have been applied regularly (Atwell et al., 2010). In *Drosophila* both RILs (King et al., 2012) and NILs (Mackay et al., 2012) have been used for genetic dissection of phenotypes. In vertebrates, mostly RILs have been relied upon and a significant number of traits have been mapped both in the rat (Pravenec, Klir, Kren, Zicha, & Kunes, 1989) and the mice (Peirce, Lu, Gu, Silver, & Williams, 2004) communities. The Mouse Collaborative Cross is the largest panel of RILs in vertebrates for complex trait analysis (Churchill et al., 2004).

With animal husbandry and long generation times being bottlenecks, so far no isogenic lines from the wild have been established in vertebrates. However, with the emergence of Medaka and its amenability to inbreeding wild catches have been collected and several laboratory strains and highly inbred strains have been established. In the recent years, a Medaka inbreeding project has been started at the Karlsruhe Institute of Technology where several Medaka wild catches are being inbred successfully (Spivakov et al., 2014). Furthermore, the process of establishing 200 lines of a Medaka isogenic panel is in progress. The typical inbreeding protocol used for Medaka is illustrated schematically in Figure 5a. In this work, several northern and southern inbred lines were used. Specifically, the northern lines are Kaga and HNI. The southern lines are HdrR, Icab, HNCMH2 and HO5. The geographical locations of these fish are shown in Figure 3a. Figure 5b shows lateral and dorsal orientations of 10 dpf Medaka hatchlings from the different inbred lines. The hatchlings show significant differences in morphology suggesting that these lines can indeed be used for

morphometric analysis and that this panel has the polymorphism that is required for GWAS.

Integrative Phenotyping: From Morphology to Behavior

As discussed before, one of the important goals of phenomics, and indeed GWAS, is to understand and relate phenotypes and genotypes. As a consequence it is essential to establish a "phenotype matrix" that consists of a host of consistent and defined parameters which can be used to characterize an individual in a population. The question then is: what formulates this phenotype matrix? In this work, we use an integrative phenotyping approach by drawing from both morphological and behavioral traits of Medaka. This simultaneous study of "form and function" is of immense importance in understanding ontogenetic and evolutionary changes and in assessing environmental effects on a population (Bertossa, 2011).

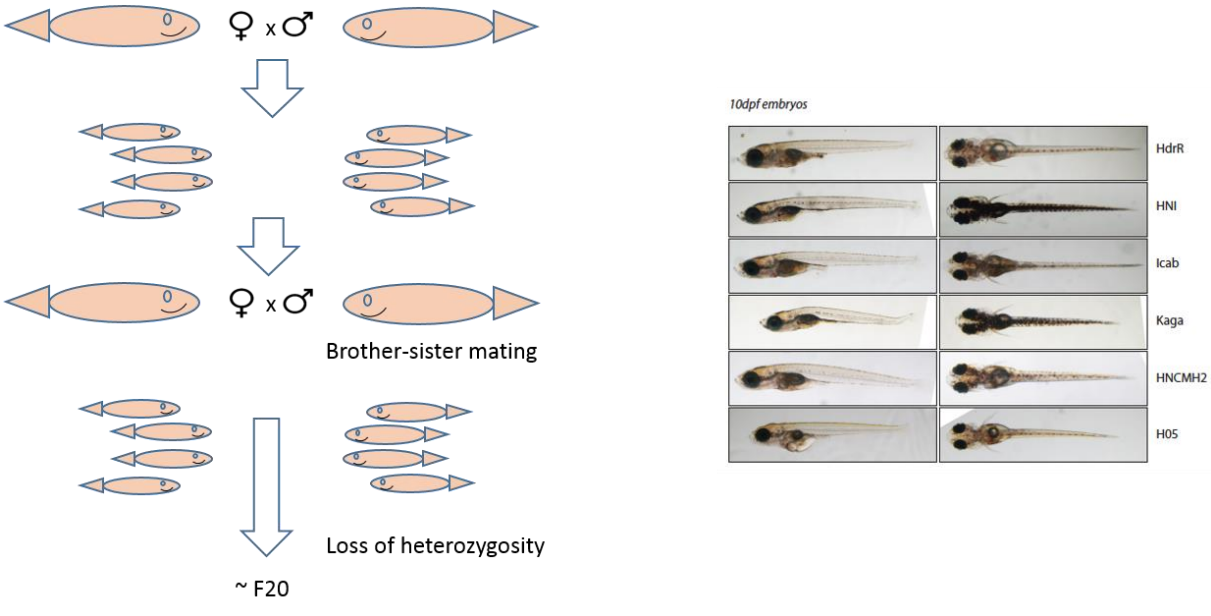

(a) (b)

Figure 5 Inbreeding (a). The inbreeding protocol. (b). Lateral and dorsal orientations of the different southern and northern inbred lines at 10 dpf.

Morphometrics

The study and analysis of size and shape and their covariance with other variables is referred to as morphometrics. The advent of fast and high-resolution imaging in the recent years combined with statistical analysis tools provide an ideal platform for the use of morphometrics in characterizing the morphology of an organism. Furthermore, since the 1980s morphometrics has changed from a qualitative science to quantitative science (Adams, 2004; Bookstein, 1998; Bookstein, Grayson, Cutting, Kim, & McCarthy, 1991; Rohlf, 1993).

There are two classical approaches to morphometrics. The first, called the 'Traditional Morphometrics', uses linear distances such as length, width and height in conjunction with multivariate statistics to assess variations in a population. While being simple, this approach has the biggest disadvantage that different shapes could produce identical measurement results because the location of the measurements is not taken into account (Rohlf, 1993). To overcome this disadvantage, landmark-based geometric morphometrics emerged. In this approach, certain specific landmarks were defined and then traditional approaches to quantify measures about the landmarks were used. In order to use this approach, the landmarks should be present in every individual of the population and if it is absent then it should either be approximately marked or not used at all (Bookstein et al., 1991; Rohlf, 1993).

Fish morphology has been studied extensively in the context of ecomorphology to evaluate the effects of habitat and environmental changes on fish (Langerhans, 2008). In Medaka, craniofacial morphology, which is a complex trait, has been studied to identify individual phenotypic differences in adult fish within the species (Kimura et al., 2007). However, to our knowledge no extensive studies of overall morphological variation in different Medaka

populations at the hatchling stage and at different developmental time points have been performed. Such a study could provide statistical data about the Medaka population diversity and could be used to understand genetic and environmental variations that contribute to the polymorphism in Medaka.

Behavior: Locomotion and Prey Capture

In order to study the complete phenotypic diversity of an organism it is important to not only understand its morphology but also its behavioral traits. Behaviors are complex traits that are controlled by a network of multiple segregating genes in response to environmental inputs (Anholt & Mackay, 2010). Organismal behavior is tuned by evolutionary forces (that tend to optimize survival and reproduction) along with developmental and physiological factors. These factors modify gene expression, neural circuitry and the interactions between them to provide an appropriate behavioral repertoire (Anholt & Mackay, 2010). A schematic diagram is shown in Figure 6 illustrating these interactions.

In vertebrates, the two most essential behavioral traits that are required by an organism for its survival are locomotion and feeding. Prey capture is an innate goal-directed behavior responsible for the feeding success of an organism. This fundamental trait manifests itself very early in an organism's developmental process. The mechanism of prey capture involves the use of specific sensory modalities and the execution of certain movements drawn from an organism's repertoire of locomotion patterns and is consequently inherently dependent on the locomotor capabilities of the organism. This behavior is controlled by several parameters including locomotor speed, maneuverability, stability, etc. Different organisms exhibit different prey capture strategies depending on the organism's morphology, physiology, environment and the nature of the prey.

Figure 7 shows schematically how these different factors influence locomotion and prey capture (Higham, 2007).

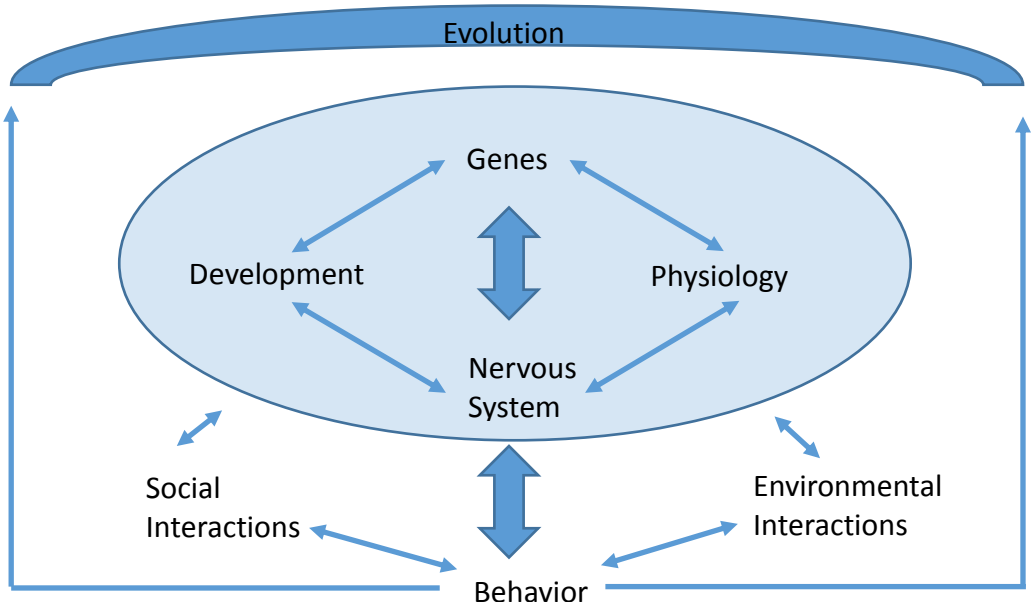

Figure 6 Evolutionary, Developmental and Physiological interactions determine behavior. Adapted from (Anholt & Mackay, 2010).

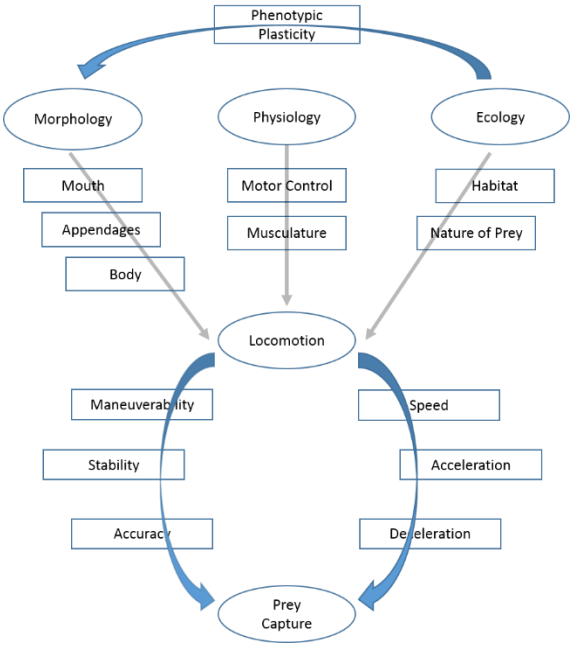

Figure 7 Factors influencing locomotion and prey capture in vertebrates. Adapted from (Higham, 2007).

Studying prey capture, therefore, allows one to dissect sensory and motor system architecture in an organism. However, the process of locomotion is extremely difficult to discern due to the complex neural structure and mechanisms. There is, consequently, the need for simple vertebrate model organisms that can be used to quantitatively assess and compare locomotor and prey capture behavior (McElligott & O'Malley D, 2005). Indeed, larval/juvenile fish have been used to study prey capture behavior and to

better understand the locomotion strategies employed for this complex behavior (Borla, Palecek, Budick, & O'Malley, 2002; McElligott & O'Malley D, 2005). Fish exhibit a variety of prey capture strategies and studying these strategies across different species can throw light on evolutionary diversity. Furthermore, a comparison between related species can provide valuable insight into the genetic principles involved in the development of these strategies (Furutani-Seiki & Wittbrodt, 2004). In this context, the zebrafish locomotion and prey capture has been extensively studied. However, to our knowledge, no study has been done to understand the locomotor and prey capture behavior in juvenile Medaka.

The zebrafish use vision as the sensory modality in prey capture (Gahtan, Tanger, & Baier, 2005). To our knowledge, there is no report on sensory modalities employed by juvenile Medaka for prey capture behavior to date. Vision based goal-directed behavior starts with target identification followed by the execution of a series of movement patterns resulting in the capture of the target (Trivedi & Bollmann, 2013). The movements themselves could be discrete or continuous in time with the aim of resolving target coordinates and trajectory and using visual feedback to finally achieve the intended goal (Land, 1992a). In recent years, several studies have been reported to understand axial kinematics and visually guided prey capture behavior in zebrafish (Bianco, Kampff, & Engert, 2011; Borla et al., 2002; Fero, Yokogawa, & Burgess, 2011; McElligott & O'Malley D, 2005; Trivedi & Bollmann, 2013).

Prey capture behavior starts to manifest itself in zebrafish around 5 dpf. Previous studies have identified the zebrafish locomotion repertoire (Fero et al., 2011) and the swimming movements and maneuvers while hunting prey. Table 2 summarizes the distinct swimming patterns that zebrafish larvae

between 5 and 7 dpf exhibit. Details of the nature of the maneuvers are also provided.

Swim Pattern	Stimulus	Details
Slow swim	Spontaneous	Also called scoots. Low tail beat amplitude; short travel distance
Burst swim	Escape response	Large amplitude tail beat; longer distances
Capture swim	Predation	Forward swim to strike at prey;
R-turn	Spontaneous	Routine turns for orientation
J-turn	Predation	Repetitive small amplitude flexion to one side; for orienting toward small prey
O-bend	Dark flash	Head of larvae meet the tail in an O-shape; low angular velocity
Short latency C-bend	Acoustic startle	Response less than 15 ms; high-angular velocity c-shape bending to one side
Long latency C-bend	Acoustic startle	Weak stimuli evoke long latency c-bending
Struggle	Trapping	When trapped, larvae show large amplitude body movements from tail towards head

Table 2 Swim pattern repertoire of zebrafish larvae between 5 and 7 dpf. (Fero et al., 2011).

The execution of the movement patterns during prey capture could be either continuous or discrete in time. An instance of the former is smooth pursuit eye movements where there is a rapid initiation of smooth eye movement followed by uninterrupted accurate tracking of the target (Lisberger, 2010). Discrete capture behavior usually consists of chaining a set of interrupted locomotion sequences by saccadic eye movements which controls gaze (Land, 1999a; Schall & Thompson, 1999; Trivedi & Bollmann, 2013).

Locomotor behavior in larval zebrafish is controlled by around 300 neurons descending from the brainstem into the spinal cord (McElligott & O'Malley D, 2005; O'Malley, Zhou, & Gahtan, 2003). Zebrafish exhibit a discrete or intermittent prey capture behavior which involves swimming bouts interspersed with pauses (Kramer, 2001; McElligott & O'Malley D, 2005). The process culminates in a capture swim when the prey is within striking distance (Borla et al., 2002). Furthermore, it is shown that the individual swimming bouts are an elementary motor pattern which is superimposed with a graded turning component (via asymmetric tail bends) controlled by visual feedback to form a goal-directed motor sequence (Trivedi & Bollmann, 2013). Importantly, it was observed that the zebrafish detect the target monocularly while the subsequent tracking and capture phases are binocular (Bianco et al., 2011; Patterson, Abraham, MacIver, & McLean, 2013; Trivedi & Bollmann, 2013).

Feeding mechanisms in fishes

Aquatic animals have to contend with several environmental factors that are significantly different from those experience by animals living on land. The density of the prey being about the same as that of water poses a special problem in that the prey often moves away from the closed mouth (Alexander, 1967). Furthermore, the density of water is $1.024 \times 10^3\ kg/m^3$ compared to

air density of $1.21\ kg/m^3$ with oxygen carrying capacity being about 95 % less than that of air. These environmental factors have contributed to the morphological evolution to improve feeding performance in fishes. The teleost cranium is of high evolutionary significance because these fishes have retained and expanded the number of joints compared to extant tetrapods (Gibb, Staab, Moran, & Ferry, 2015; Hulsey, Fraser, & Streelman, 2005; Liem, Bemis, Walker, & Grande, 2001). The teleost skull is made of up of more than 100 bones that act as functional units and are able to move relative to one another with the primary functions of respiration and feeding (Gibb et al., 2015). This is contrast to 44 bony elements at birth and 22 bones at adulthood in humans. In addition, the human skull shows very little kinesis.

Three important categories into which fish feeding mechanisms can be divided are:

1. Suction feeding
2. Ram feeding
3. Manipulation

These three categories are not mutually exclusive (Liem, 1980). Suction feeding functions via the generation of a pressure gradient between the inside of the buccal cavity and the surrounding water caused by a rapid expansion of the oral cavity. This causes the water to flow into the mouth carrying the prey that is engulfed in the water current. Ram feeding is accomplished by the fish overtaking the prey through forward body movements. While in suction feeding the prey is consumed via the water current created by the fish, in ram feeding the mouth of the fish is thrust or rammed over the prey. Suction and ram feeding exist as the extremes of a feeding modality continuum (Norton & Brainerd, 1993; Wainwright, 1999). Finally, manipulation feeding involves variations in the use of oral jaws to grasp prey. It involves the application of the

oral jaws to the prey and biting the prey off a substrate or making pieces out of a large prey (Wainwright, 1999). It is believed that all fish species use one or a combination of these three fundamental modes of feeding. Furthermore, the mode (or modes) used reveal the relationship between craniofacial structure, and indeed morphological specialization, and the nature of the prey (Liem, 1980; Wainwright, 1999).

Objectives

Morphology and behavior are two key traits that can be used to understand the interactions between the genotype, the environment and the phenotype. The aim of this thesis is to establish a framework to identify and quantify appropriate morphological and behavioral phenotypes using representative northern and southern inbred Medaka lines. This framework will subsequently be used to systematically phenotype more than 200 inbred Medaka lines and use the resulting phenotypic matrix for GWAS.

For morphometry, the thesis will address:

- Establishing a protocol for extracting gross morphological features
- Comparison of the morphological features of the different lines at two time points: 10 dpf and 20 dpf
- Identifying key features that show significant differences among the different lines

The second part of the thesis focusses on behavioral phenotyping and will address:

- Establishing systems and algorithms for quantitative assessment of behavior
- Evaluation of locomotion in Medaka
- Prey capture behavior in Medaka
- Comparison of prey capture behavior with zebrafish to understand interspecific strategies
- Comparison of prey capture behavior among the different Medaka lines to understand variation in strategies within a population

Methods

Fish Stocks and Husbandry

The following Medaka lines were used for morphometric and behavioral analysis:

- Northern lines: HNI and Kaga
- Southern lines: HdrR, Icab, HNCMH2 and HO5
- 2 sets of Trios

The geographical locations of these lines are shown in Figure 3a. The strains were obtained from the National Institute of Basic Biology (NIBB), Japan, and raised at the Karlsruhe Institute of Technology, Germany. The HdrR lines were generated by from the d-rR line (Yamamoto, 1953) established from commercial orange-red and white varieties from unknown locations. However, phylogenetic analysis has confirmed that the HdrR belongs to the Southern Japanese population (Spivakov et al., 2014). The HNI (Northern Japanese population) was established from a wild collection from Niigata city, Niigata Prefecture, Japan. The northern Kaga strain was established from wild population collected at Kaga, Ishikawa Prefecture, Japan. The southern Icab and HNCMH2 were purchased from Carolina Biological Supply (Burlington, NC) and were established from Southern Japanese populations with more than 20 generations of inbreeding (Spivakov et al., 2014). All the lines were kept and raised under 14 h light/10 h dark conditions at 26 °C. The embryos were kept in a 1 x hatching medium (0.1% NaCl, 0.003% KCl, 0.004% $CaCl_2$, 0.016% $MgSO_4$, 0.0001% Methylene blue) until hatching (Loosli et al., 2000).

Zebrafish were maintained and bred using conditions described in (Westerfield, 2007). Embryos were raised in embryo medium at 27 °C under 14 h light/10 h

dark cycles. Wild type ABTL zebrafish larvae at 6 – 8 dpf were used. The zebrafish lines were maintained at the Max Planck Institute for Medical Research, Heidelberg, Germany.

Animal husbandry and experiments were performed in accordance with the German law on Animal Protection which was approved by the Regierungspräsidium Karlsruhe (Local Animal-Protection Committee), Az. 35-9185.64.

Morphometry

Morphological features from the four southern lines, the two northern lines and the trios were analyzed. The embryos from all the lines were raised under identical conditions.

Imaging

The imaging of the different lines was performed with hatchlings at 10 dpf. Healthy individuals were transferred to a petri dish with fresh fish water. They were then anesthetized using Tricaine mesylate (MS-222). The hatchlings were then individually mounted in 85% glycerol. They were then manually oriented to dorsal or lateral orientations. The imaging itself was performed using a Leica MZ 16 FA stereomicroscope with a Planapo 1.0 x objective and a 10 (for 20 dpf hatchlings) or 20 x (for 10 dpf hatchlings) zoom factor. Typical dorsal and lateral orientation images are shown in Figures 8a and 8b.

(a)

(b)

Figure 8 Typical examples of hatchlings for morphometric imaging. (a). Dorsal orientation. (b). Lateral orientation.

The images obtained from both orientations were then analyzed using a semi-automated and a completely automated algorithm. The intent was to compare and verify the accuracy of the automated algorithm read-outs with the read-outs from the semi-automated version. This automated algorithm will be used in the future for quantifying the morphological features of the entire 200 inbred lines panel.

Semi-automated algorithm for quantifying features

In this approach, the landmarks are selected manually from the microscopy images of the hatchlings from the two orientations. The images are presented to the user via a Graphical User Interface (GUI) and the user is prompted to select the "points" that define the landmarks. Each landmark is associated with two points. The morphometric feature is then the Euclidean distance between the two points. For example, let one landmark (say the total body length) be defined by two points: $p_1 = (x_1, y_1)$ and $p_2 = (x_2, y_2)$. The Euclidean distance between the two points is then:

$$\mathbf{d}(p_1, p_2) = \sqrt{(x_2 - x_1)^2 + (y_2 - y_1)^2} \qquad (2)$$

After all the points of the landmarks have been entered via the GUI, the algorithm computes the respective landmark features and writes it to a file. The various features for the different lines and orientations are then statistically analyzed. The GUI and the algorithm was programmed using MATLAB (The Mathworks Inc., Natick, Massachusetts) (Peravali et al., 2011; Sinn, Peravali, Heermann, & Wittbrodt, 2014; Spivakov et al., 2014). Figure 9 shows the GUI with an example of landmark selection.

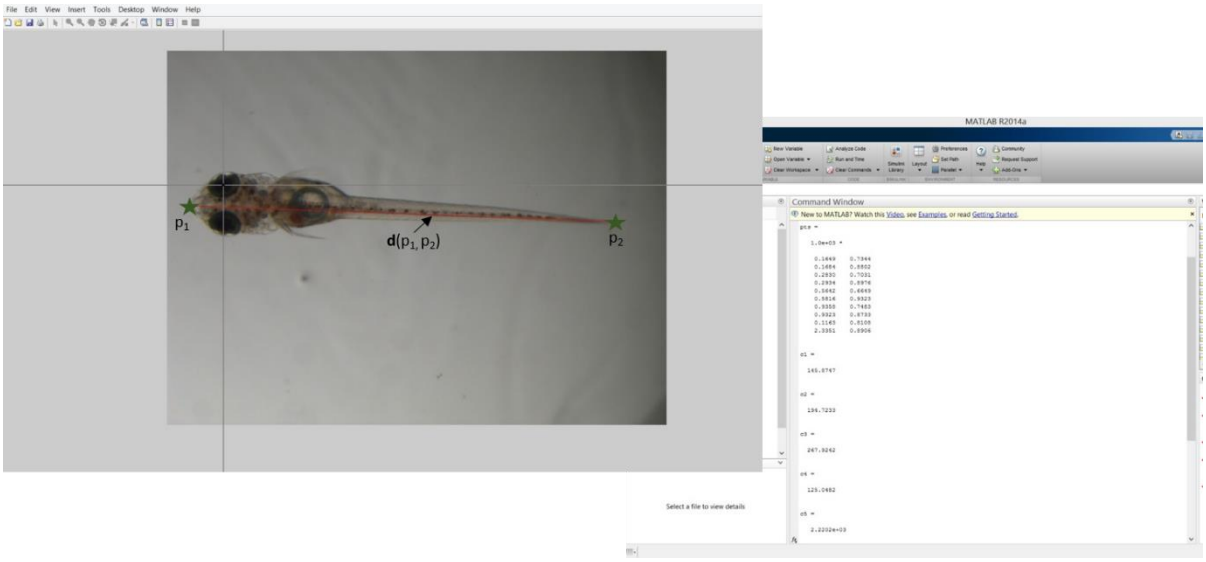

Figure 9 Graphical User Interface for the semi-automatic method of computing morphometric features. The GUI allows the user to choose the landmarks and then quantifies them.

Automated approach to feature extraction and quantification

For high-throughput phenotyping and quantification of morphometric features, the semi-automated approach is unsuitable. It is especially cumbersome to use this approach as the goal is to extract the morphometric features from a large number of individuals from 200 inbred lines in the future. Consequently, an automated algorithm was developed to avoid manual selection of the landmarks and provide an interface that automatically extracts the features and quantifies them. The developed algorithm is shown schematically in Figure 10 and the steps comprising the algorithm are discussed individually. The algorithm was implement in MATLAB (The Mathworks Inc., Natick, Massachusetts).

Step 1: The image obtained from the microscope is in the RGB format which is an additive color model with red, blue and green as the primary colors (Gonzalez & Woods, 2002). The size of the image is 1944 pixels x 2592 pixels.

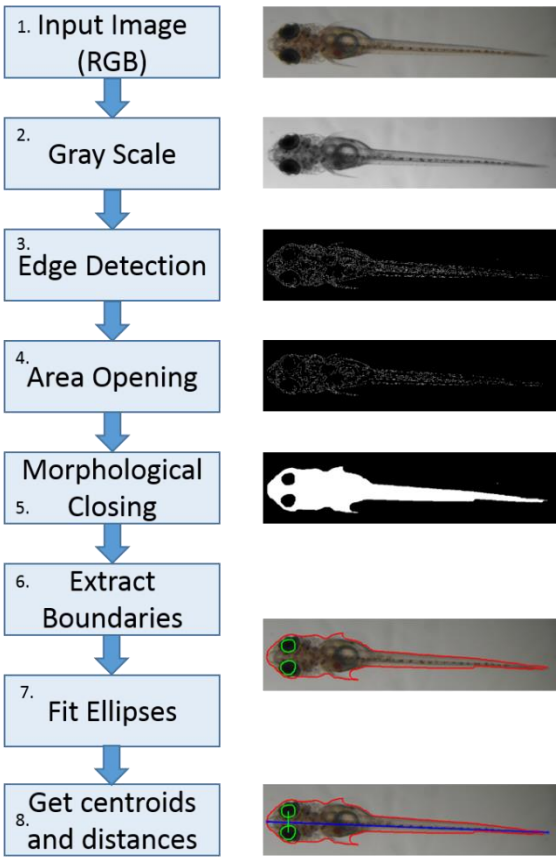

Figure 10 Automated algorithm to morphometric feature extraction and quantification. Left panel shows the algorithm flow. Right panel shows cropped versions of the images at each step of the algorithm.

Step 2: In order to improve the processing speed for extracting the morphological features, the RGB image was converted to a grayscale image. The grayscale images are obtained by eliminating hue and saturation data while retaining the luminance information (MATLAB and Image Processing Toolbox™). The grayscale values are computed as a weighted sum of the R, G, and B components according to (Poynton, 1996):

$$Grayscale\ value = 0.2989 \times R + 0.5870 \times G + 0.1140 \times B. \quad (3)$$

The grayscale image is converted to an intensity image with values in the range [0, 1] by normalizing the grayscale values by the maximum possible grayscale value of 255.

Step 3: The image obtained from the previous step is then used to extract edge information. Edge detection identifies points of discontinuous brightness in an

image and connects and represents them via curved line segments. In the algorithm, the Canny edge detector is used (MATLAB and Image Processing Toolbox™). The Canny detector is an optimal detector that finds the edges using the local maxima of the gradient of the image in the horizontal and vertical directions. The gradient itself is found using the derivative of a Gaussian filter and the gradient direction is perpendicular to the edges. The detector uses a method called "feature synthesis" that integrates edge information from fine-to-coarse scale using two thresholds: the high and low thresholds. All edges above the high value are sure to be edges, while those below the low values are discarded as non-edges. Values between the two thresholds are considered edges only if they are connected to the "sure-edges". This makes the detector robust to noise and other spurious effects due to non-uniform illumination, etc. (Bradski & Kaehler, 2008; Canny, 1986). In the algorithm, a Gaussian filter of size 7 with standard deviation $\sigma = \sqrt{2}$ is used with the thresholds being [0.15, 0.6]. The resulting edge image is binary with values 1 representing the edges and the rest of the image values being 0.

Step 4: In order to further improve the edge image and retain only relevant edge information a method known as area opening is applied to the binary edge image obtained in Step 3. Area opening removes those connected components (essentially objects) in a binary image whose area is smaller than a parameter λ (Vincent, 1993). In the algorithm, connected components are labeled using 8-connectivity neighborhood: that is, pixels are said to be connected if their edges or corners touch. This means that if two adjoining pixels have value 1 in a binary image, then they are considered as part of the same object irrespective of whether they are connected horizontally, vertically or diagonally (Cheng, Peng, & Hwang, 2009) . All such objects in the image that have fewer than 10 pixels are removed.

Step 5: The image obtained in the above step has all the details of the landmarks (via the edge information) but still lacks continuity that is required for quantification. Morphological closing is an important operator applied to binary images to enlarge foreground boundaries (bright regions) while shrinking the background holes in these regions. It, however, preserves the original boundary shape (Gonzalez & Woods, 2002). It functions by using a structuring element which defines a particular shape and the closing operator then preserves regions that are similar to the shape descriptor in the image while eliminating other regions. As can be seen in the right panel of Figure 11, the closing operator extracts the elliptical shape of the eyes and the outer boundary which are required for the quantification of the morphometric features. In the algorithm, the structural element was a disk (elliptical shape) of radius 35. This shape descriptor was found to be optimal in extracting all relevant features in the hatchling image.

Steps 6, 7 and 8: Once the contours of the outer boundary and the eyes have been obtained from the previous step, the algorithm quantifies the various landmarks. Firstly, the pixel coordinates (X, Y) of the outer boundary and the eyes are extracted. The perimeters and the areas of these different regions are then estimated. The region corresponding to the maximum area is the outer boundary and the regions with smaller areas are the eyes. For the eyes, the centroids of the ellipses fitting the coordinates are computed and the distance between the centroids is then evaluated. For the other landmarks, the extrema of the coordinates are computed and the distance between them are evaluated.

The algorithm described above was implemented in MATLAB with the Image Processing Toolbox™ and parts of it are reported in (Herder et al., 2013; Peravali et al., 2011; Sinn et al., 2014; Spivakov et al., 2014).

Behavior

Three behavioral traits are evaluated in the Medaka inbred lines: locomotion, feeding and prey capture. Imaging platforms are developed for acquiring behavioral data and algorithms are developed to quantify this data. For the feeding and prey capture experiments the hatchlings were fed with *Paramecium caudatum.*

Imaging: Locomotion and Feeding

In order to observe locomotion and feeding behavior, an automated system that is capable of imaging Medaka hatchlings over long periods of time is essential. Furthermore, the imaging resolution should be high enough to detect the hatchling and the paramecia in the acquired data. Accordingly a high-throughput robotic imaging platform was developed to acquire video data of the hatchlings. The platform is shown in Figure 11 and consists of four essential elements. The first is a TX40 6-axis Stäubli robotic arm (Stäubli Tec-Systems GmbH, Germany). This is an articulated arm that provides high precision, high flexibility and high speed operability. The arm has 6 degrees of freedom and a reach at the wrist of 515 mm and a repeatability of ± 0.02 mm. Its wrist consists of a gripper that can carry loads of up to 2.3 kg. Such an arm has the advantage of maximal utilization of workspace that contributes towards a high-throughput performance.

In order to observe locomotion and feeding behavior, an automated system that is capable of imaging Medaka hatchlings over long periods of time is essential. Furthermore, the imaging resolution should be high enough to detect the hatchling and the paramecia in the acquired data. Accordingly a high-throughput robotic imaging platform was developed to acquire video data of the hatchlings. The platform is shown in Figure 11 and consists of four essential elements. The first is a TX40 6-axis Stäubli robotic arm (Stäubli Tec-Systems

GmbH, Germany). This is an articulated arm that provides high precision, high flexibility and high speed operability. The arm has 6 degrees of freedom and a reach at the wrist of 515 mm and a repeatability of ± 0.02 mm. Its wrist consists of a gripper that can carry loads of up to 2.3 kg. Such an arm has the advantage of maximal utilization of workspace that contributes towards a high-throughput performance. The second component is the imaging sensor. For this a 1.3 megapixel CMOS sensor called the UI-1540SE (from iDS Imaging Development Systems GmbH, Germany) is used. This sensor provides up to 25.0 frames per second recording capability and offers a resolution of 1280 × 1024 pixels. The large pixels produce an extremely good signal-to-noise ratio and consequently a high image dynamic. The third component is a dark field illumination setup that was designed to provide better contrast of hatchlings and the paramecia in the acquired videos. The setup allows for 12 petri-dishes of 3.5 cm diameter to be positioned in 4 rows. Due to the flexibility of the robot arm, the number of petri-dishes can be scaled up to a significantly larger number in the future. Finally, the fourth component is the petri-dishes themselves. A magnified image of a typical petri-dish containing one hatchling and paramecia is shown on the right side of the Figure 11. The whole system is mounted on an optical table to provide vibration isolation and is enclosed in a temperature controlled chamber that maintains the temperature at 29 °C. Once the petri-dishes containing the hatchlings (and the paramecia, if required) are positioned on the

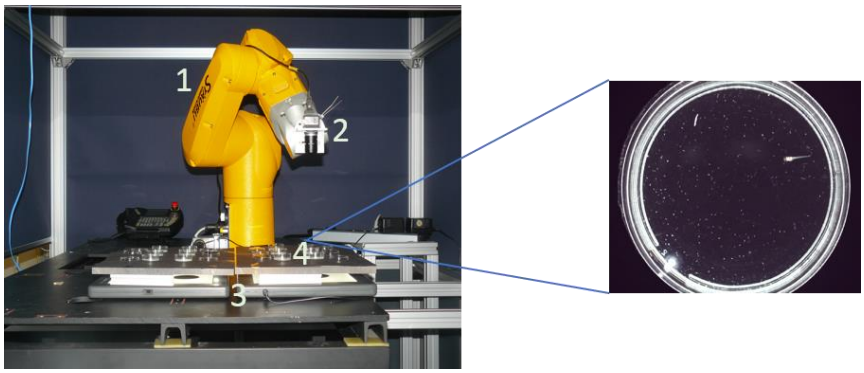

Figure 11 Robotic imaging platform for locomotion and feeding behavior studies. 1. Robotic arm. 2. Camera functioning at 25 fps. 3. Dark field setup. 4. Petri-dishes with hatchlings and the magnified view.

dark field setup, the robot arm positions the imaging sensor over the top of first petri-dish. Video of the hatchling activity is then recorded. The robot arm then moves to the next positions sequentially and repeats the recording over each petri-dish. After all the 12 petri-dishes have been recorded, the arm moves back to the first position and repeats the process all over again.

Experiment Protocol: For locomotion experiments, Medaka hatchlings at 10 dpf are used. The hatchlings are transferred to petri-dishes containing 5 ml of fish water. They are allowed to acclimatize for 1 hour before the start of the experiment. For feeding experiments, Medaka hatchlings at 10 dpf are transferred to petri-dishes with 4 ml of fish water, one hatchling per petri-dish. 1 ml solution with paramecia is then added to the petri-dishes. The density of the paramecia is adjusted to be 100 paramecia per ml. One control petri-dish with 4 ml of fish water and 1 ml of the paramecia solution is used in every feeding experiment. For both the locomotion and feeding experiments, videos of 3 minute duration per petri-dish are acquired every 36 minutes for 3 hours. This gives 6 independent recordings of activity for each petri-dish. In order to account for time-of-day influences, if any, the experiments were performed once in the morning (09:00 hours to 12:00 hours), once after noon (13:00 hours to 16:00 hours) and once in the evening (17:00 hours to 20:00 hours). For feeding experiments, the 3 time point's repeats were performed on 3 different days using hatchlings of the same age and developmental stage in order to avoid the influence of food intake at one time point on the others.

Automated tracking of Medaka hatchlings

To assess locomotion in Medaka hatchlings, the videos acquired using the imaging platform described above are automatically analyzed to extract locomotion tracks and to quantify locomotion parameters: speed of movement and the distance travelled in a given time. The algorithm developed to achieve

this task is shown in Figure 12 and is based on frame differencing which has played an important role in many computer vision applications like compression, surveillance, etc. (Zeng, Gao, & Zhao, 2003). The first step in the procedure is to set the first frame in the video as a reference frame. Following this, the subsequent frames are read-in sequentially. In order to detect motion, each subsequent frame is subtracted from the reference frame pixel-by-pixel. This difference image is then converted to gray scale (similar to Step 2 in Figure 10) and thresholded to improve the quality of the difference image. If there indeed was motion between the two frames, the difference image will then have intensity values only at those pixel locations where change occurred due to the motion. This will then result in a non-zero difference image. Subsequently, all non-zero components in the image are labelled similar to the procedure described in Step 4 of Figure 10.

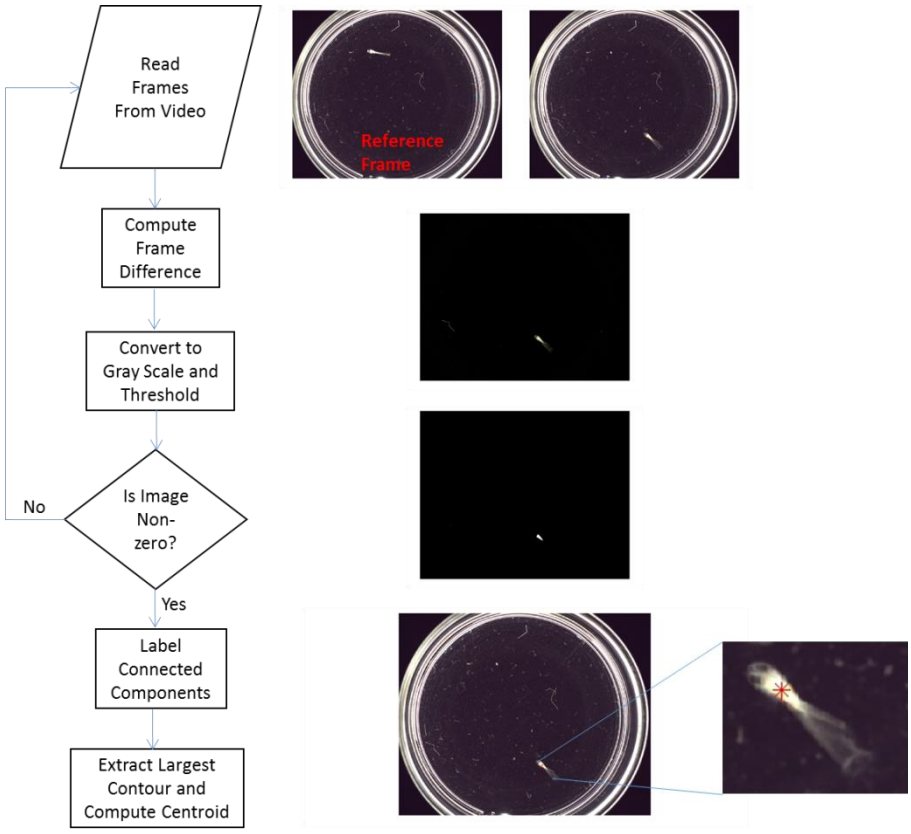

Figure 12 Algorithm to track Medaka hatchlings to assess locomotion behavior. Left panel shows the algorithm flow and the right panel images at each step of the algorithm.

The largest contour in this labelled image will correspond to the contour of the hatchling and is extracted. The centroid of this contour is then calculated. This process is repeated over all the frames in the video resulting in a list of centroids of the hatchling at its various positions.

The temporal change in the centroid coordinates yields the locomotion track and can then be used to extract the distance travelled and the speed.

Automated algorithm to quantify feeding behavior

The rate at which different Medaka hatchlings from different lines consume paramecia in a given time is used as a measure to quantify feeding behavior. Since manual computation of the number of paramecia consumed over time is time-consuming and error prone, an automated algorithm to achieve this was developed. This algorithm essentially counts the number of paramecia at different time points during the course of the experiment. The rate is then computed as the number of paramecia consumed as a function of time. The algorithm is shown schematically in the left column of Figure 13. The middle and right columns of the figure show the detection and extraction of paramecia from the videos at two different time points.

The algorithm uses several components from the other algorithms described above and is therefore only briefly described here. The algorithm begins by extracting individual frames from the acquired videos of 3 minute duration. Since the well geometry and position is known *a-priori*, each image is cropped automatically to obtain only the relevant regions-of-interest. This operation is useful as the dimension of the paramecia is very small within the field-of-view and the edges of the petri-dish may introduce false positives. The cropped image is then binarized, filtered and the connected components are labelled similar to the algorithms described above. Finally the centroids of the detected paramecia are computed and the number calculated.

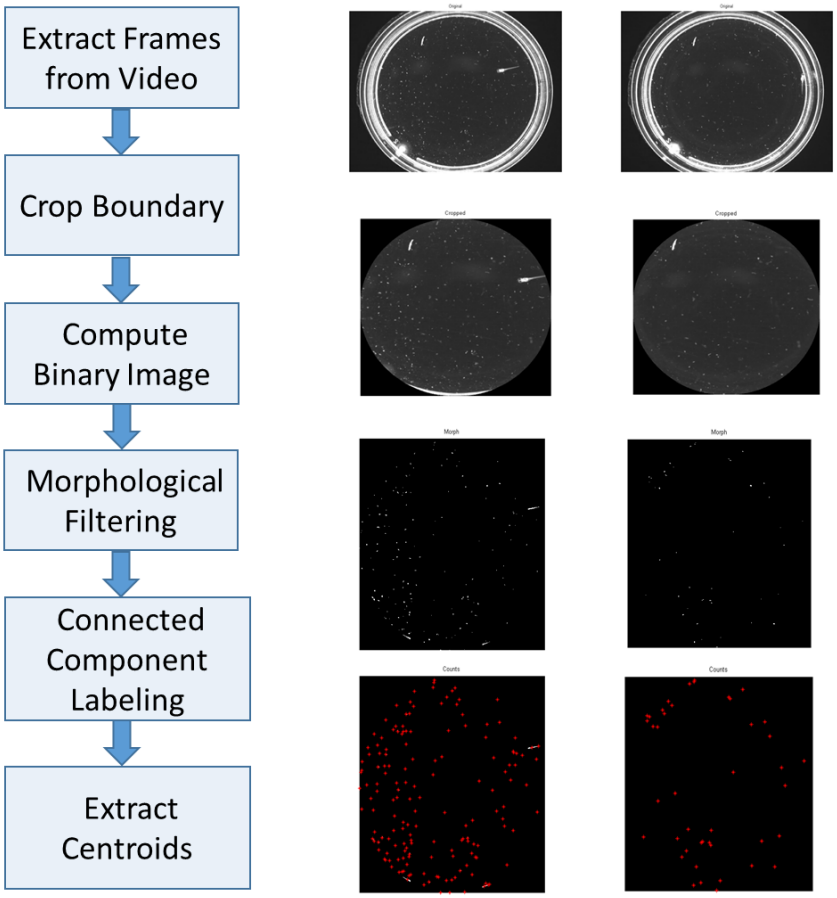

Figure 13 Algorithm to assess feeding behavior. Left panel shows the analysis steps and the right panel representative images at each step.

All algorithms described above were implemented in MATLAB with the Image Processing Toolbox™.

Imaging: Prey Capture Studies

For prey capture studies, the HNI (northern line) and the HO5 (southern line) strains of Medaka hatchlings at 10 dpf and zebrafish larvae at 6 – 8 dpf were used. At this age, the Medaka and zebrafish larvae have similar size, are free-swimming and capture paramecia successfully for feeding. The imaging setup used to study prey capture was identical to the system reported in (Trivedi & Bollmann, 2013) and is shown schematically in Figure 14.

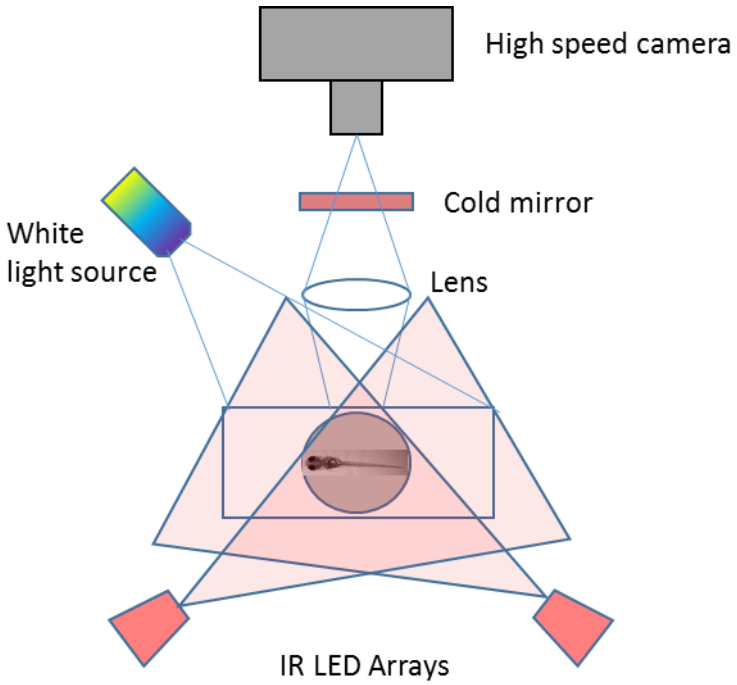

Figure 14 Experimental setup for prey capture studies. Adapted from (Trivedi & Bollmann, 2013) .

The larvae are imaged in a small petri-dish of 16 mm diameter and 5 mm height with a transparent bottom and opaque walls and with 3 – 4 mm of fish water. The dish contains a single larva which is provided with a single paramecium to capture. The arena is illuminated with white light from the top and an array of

three infra-red LEDs (Kingbright, BLO-106) are mounted beneath to record the larvae and the paramecium under dark-field illumination. A high-speed camera (AOS Imaging Systems, Model S-PRI 1039) is used to record the prey capture sequence. A cold mirror is mounted to block white light from the camera. All prey capture sequences were recorded at 250 frames/second and the experiments were conducted at room temperature.

Image analysis: Prey capture studies

The video recordings obtained from the imaging system above are in the 8-bit grayscale format and are processed to extract different parameters of the prey capture sequence. Figure 15 shows the different parameters that are extracted and quantified. The image analysis is performed using the software developed in (Trivedi & Bollmann, 2013). To facilitate the analysis, the paramecium is initially identified manually in the first frame. After this, the tracking of the fish and the paramecium is done automatically.

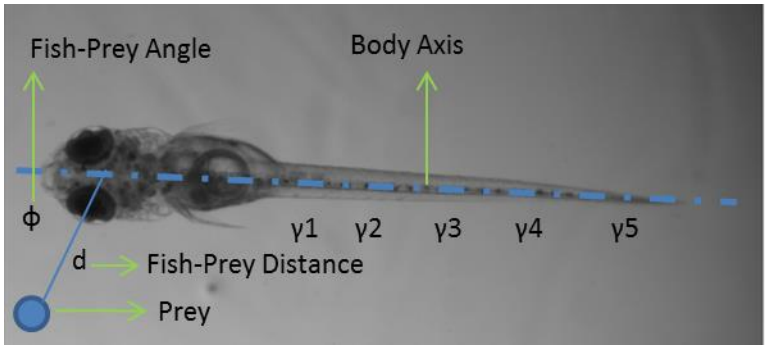

Figure 15 Parameters extracted from the prey capture sequences.

The algorithm determines the midline of the fish which is composed of 6 segments. The first segment is the head segment measured between the snout and the swim bladder. The rest of the midline is split into 5 line segments of equal length. The tail movements during the prey capture are quantified as angles ($\gamma_{1,\ldots,}\gamma_5$) which are the angles between the 5 individual tail segments

and the body axis (the heading direction of the first segment). With respect to a global reference plane, the orientation of the fish, Θ, is the angle of the head segment of the midline. For each frame, the angle between the fish and the paramecium (the fish-target angle, ϕ) is calculated. Furthermore, the fish-target distance, d, is computed as the distance between the center of the head segment of the midline and the centroid of the paramecium.

To record the entire prey capture sequence, a large field-of-view was used. This, however, does not allow for automatic analysis of smaller details and consequently the ipsilateral and contralateral eye angles with respect to the midline and the prey were analyzed manually. The prey capture trajectories were plotted using the centroids of the detected fish in each frame.

Results

Morphometrics

The aim of morphometric analysis was to identify and quantify landmarks that could be used to distinguish between the different lines of the inbred Medaka panel. The landmarks were measured at two developmental time points: 10 dpf and 20 dpf. Furthermore, one southern inbred line (HO5) and one inbred northern line (HNI) were chosen as representatives for comparisons. Some lines were not included for analysis at 20 dpf due to lack of enough hatchlings at this time point. For each landmark, box plots of the data are shown and p-value indicating significant differences or not between HO5 and HNI are shown for each time point. The outliers are indicated as red crosses. Tables are also provided to show the basic statistics of the data.

Morphological Landmarks

For each orientation of the larva, several gross morphological landmarks were identified. Specifically, for the dorsal orientation the following landmarks were chosen:

1. Lip width
2. Distance between the eyes
3. Dorsal width (just near the pectoral fins)
4. Width just beyond the yolk sac and at the start of the yolk extension
5. Dorsal length

For the lateral orientation the following landmarks were chosen:

1. Eye diameter
2. Lateral width before the start of the yolk sac
3. Point of maximal lateral width

4. Lateral length

Figures 16a and 16b show these landmarks. These features were chosen as they offered the most distinguishable differences between the various lines on observation. The lengths are “total lengths” measured from the tip of the mouth at the anterior end to the tip of the caudal fin at the posterior end. Since in fish variations in individuals correlate with body length, the different features were normalized by the total body length.

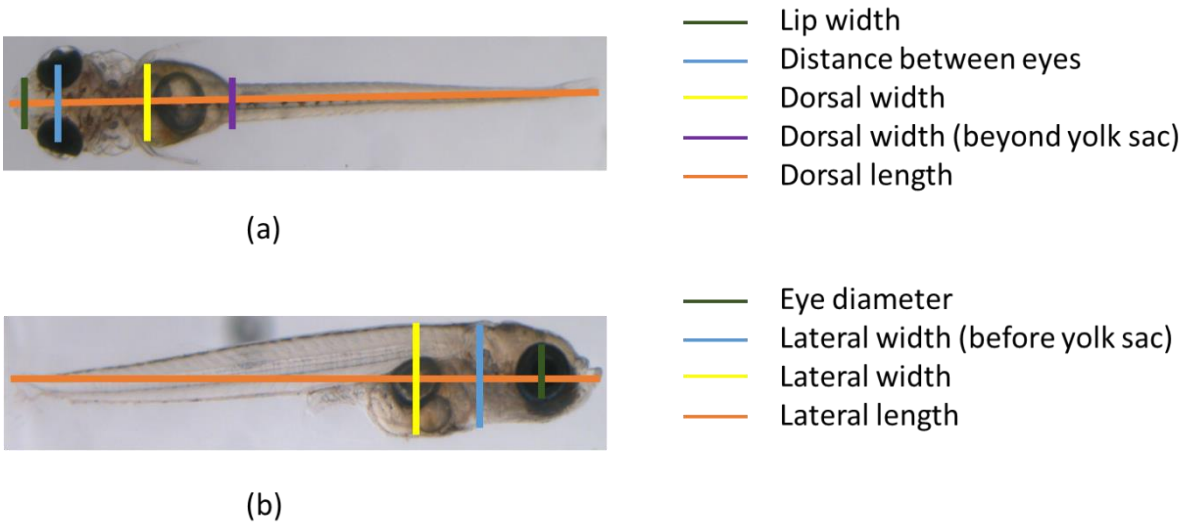

Figure 16 Morphometric landmarks. (a). Dorsal landmarks (b). Lateral landmarks.

Dorsal lip width normalized to dorsal length

The lip width is the length of the mouth of the hatchlings seen from the dorsal orientation. Figure 17 shows the lip widths of the different inbred lines. Table 3 provides the relevant statistics. While some lines show similar lip widths although they are from different regions (HdRr and Kaga), the HO5 and HNI lines show significant differences both at 10 dpf ($p << 0.01$) and at 20 dpf ($p <<< 0.001$). Furthermore, there are differences between the southern lines (Icab, HO5 and Hncmh2). The differences in the lip widths between southern and northern lines gets significantly more at 20 dpf.

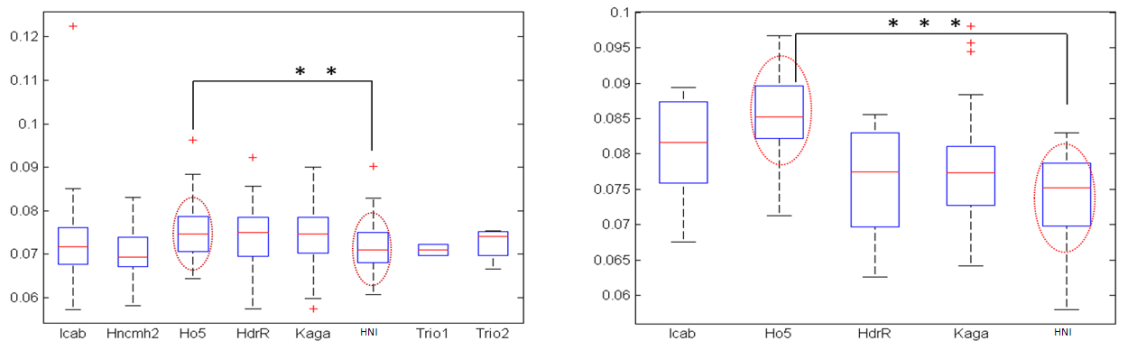

(a) (b)

Figure 17 Dorsal lip width normalized to dorsal length. (a). Comparison at 10 dpf showing significant differences between HO5 and HNI lines. (b). Comparison at 20 dpf. Very significant differences are seen between HO5 and HNI lines. Differences are also noticed among the southern lines.

	Sample Size	Mean	Median	Standard Deviation
Icab	79	0.0721	0.0717	0.0084
Hncmh2	16	0.07	0.0692	0.0061
HO5	53	0.075	0.0746	0.0068
HdrR	76	0.0739	0.075	0.0066
Kaga	122	0.0747	0.0747	0.0072
HNI	46	0.0713	0.071	0.0061
Trio 1	2	0.071	0.071	0.0018
Trio 2	4	0.0725	0.074	0.0041

(a)

	Sample Size	Mean	Median	Standard Deviation
Icab	24	0.0812	0.0816	0.0064
HO5	25	0.0856	0.0852	0.0065
HdrR	16	0.0758	0.0775	0.0078
Kaga	49	0.0773	0.0773	0.0074
HNI	23	0.0737	0.0752	0.0069

(b)

Table 3 Dorsal lip width statistics. (a). At 10 dpf. (b). At 20 dpf.

Distance between eyes normalized to dorsal length

The second dorsal landmark that was quantified was the distance between the eyes measured from the dorsal orientation and is an important craniofacial landmark. This is the distance between the centroids of the ellipses fitted to the two eyes. This feature plays an important role in the visual mechanism of the fish. Figure 18 and Table 4 show the relevant measurements.

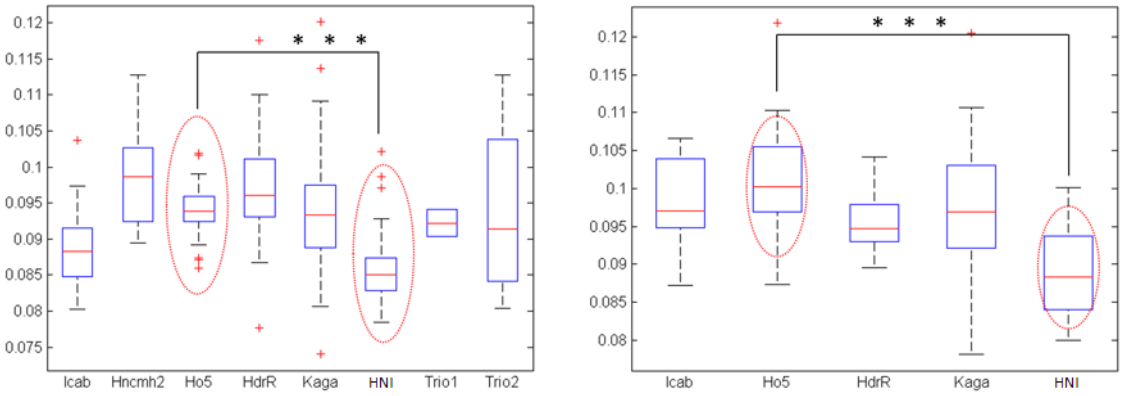

Figure 18 Distance between the eyes normalized to dorsal length. (a). At 10 dpf. (b). At 20 dpf. Significant differences are observed between HO5 and HNI at both stages. There are significant differences between all the southern lines at 10 dpf which tends to become smaller at 20 dpf.

	Sample Size	Mean	Median	Standard Deviation
Icab	79	0.0886	0.0882	0.0049
Hncmh2	16	0.09876	0.0988	0.0073
HO5	53	0.094	0.094	0.0033
HdrR	76	0.0971	0.0961	0.0059
Kaga	122	0.0935	0.0933	0.0069
HNI	46	0.0861	0.085	0.005
Trio 1	2	0.0922	0.0922	0.0027
Trio 2	4	0.094	0.0914	0.0139

(a)

	Sample Size	Mean	Median	Standard Deviation
Icab	24	0.0978	0.0970	0.0061
HO5	25	0.1014	0.1003	0.0074
HdrR	16	0.0958	0.0947	0.0038
Kaga	49	0.0976	0.0969	0.0080
HNI	23	0.0889	0.0883	0.0058

(b)

Table 4 Distance between eyes measured from dorsal orientation. (a). At 10 dpf. (b). At 20 dpf.

The differences between the HO5 and HNI lines are very significant (p <<< 0.001) at both 10 and 20 dpf. Interestingly, all the southern lines show significant differences from each other at 10 dpf (with Icab and HdrR showing the most variation). However, at 20 dpf this difference tends to get smaller. Furthermore, the lines show an increase in the distance with age.

Dorsal width normalized to dorsal length

Two dorsal widths are used as landmarks. The first is the width of the hatchling measured between the pectoral fins. Figure 19 and Table 5 describe the landmark.

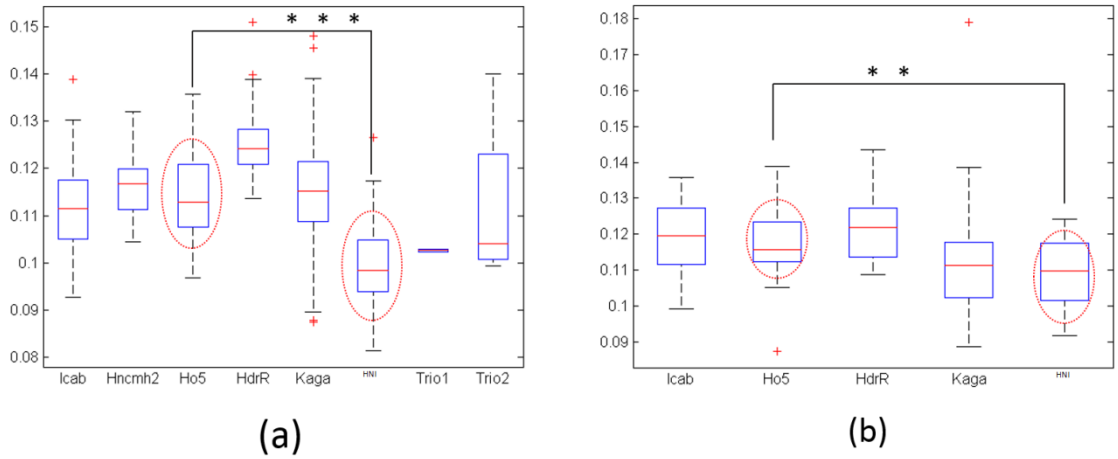

Figure 19 Dorsal width normalized to the dorsal length. (a). At 10 dpf. (b). At 20 dpf. Significant differences are observed among the different lines at 10 dpf and the differences get reduced at 20 dpf. HO5 and HNI show differences at both time points.

As in the case of the distance between the eyes, the dorsal width between the pectoral fins showed variations among the southern and the northern lines. At 10 dpf the difference between HO5 and HNI was very significant (p <<< 0.001) and at 20 dpf the difference was significant (p << 0.001). At 10 dpf the Icab and HdrR southern lines show maximum difference in width which becomes less pronounced at 20 dpf.

	Sample Size	Mean	Median	Standard Deviation
Icab	79	0.1111	0.1115	0.0089
Hncmh2	16	0.1167	0.1167	0.0071
HO5	53	0.1141	0.1128	0.0086
HdrR	76	0.1249	0.1241	0.0063
Kaga	122	0.1153	0.1151	0.0112
HNI	46	0.0999	0.0984	0.0089
Trio 1	2	0.1027	0.1026	0.0003
Trio 2	4	0.1119	0.104	0.019

(a)

	Sample Size	Mean	Median	Standard Deviation
Icab	24	0.1189	0.1196	0.0099
HO5	25	0.1175	0.1157	0.0105
HdrR	16	0.1221	0.1218	0.0093
Kaga	49	0.1129	0.1113	0.0147
HNI	23	0.1094	0.1099	0.0095

(b)

Table 5 Dorsal width normalized to the dorsal length. (a). At 10 dpf. (b). At 20 dpf.

Dorsal width beyond the yolk sac normalized to dorsal length

The second dorsal width landmark was measured just beyond the yolk sac.

Figure 20 and Table 6 show the statistical data.

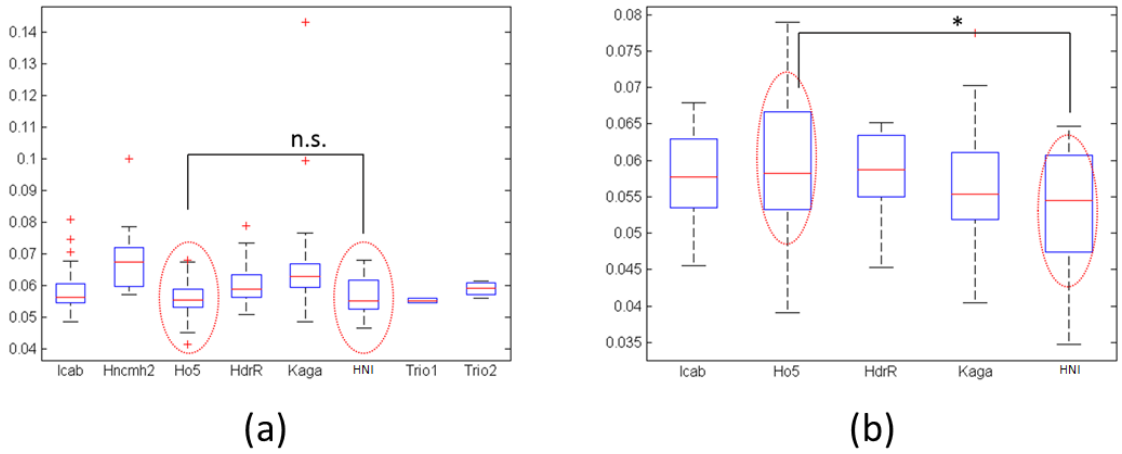

Figure 20 Dorsal width beyond the yolk sac normalized to the dorsal length. (a). At 10 dpf. (b) At 20 dpf. There is no significant difference between the lines at both time points. The width remains approximately same at both 10 and 20 dpf.

	Sample Size	Mean	Median	Standard Deviation
Icab	79	0.0576	0.0563	0.0057
Hncmh2	16	0.0683	0.0673	0.0106
HO5	53	0.0556	0.0552	0.0049
HdrR	76	0.0597	0.0588	0.0052
Kaga	122	0.0639	0.0627	0.0096
HNI	46	0.0562	0.0551	0.0057
Trio 1	2	0.0550	0.0550	9.7504e-04
Trio 2	4	0.0588	0.0590	0.0024

(a)

	Sample Size	Mean	Median	Standard Deviation
Icab	24	0.0578	0.0578	0.0059
HO5	25	0.0599	0.0582	0.0094
HdrR	16	0.0582	0.0587	0.0059
Kaga	49	0.0565	0.0554	0.0070
HNI	23	0.0530	0.0545	0.0095

(b)

Table 6 Dorsal width beyond the yolk sac normalized to the dorsal length. (a). At 10 dpf. (2). At 20 dpf.

There are no significant differences between the different lines for this landmark at 10 dpf. However, at 20 dpf, differences between the northern and southern lines emerge and specifically between the HO5 line and the HNI line ($p < 0.05$).

Dorsal length

The dorsal length is measured from the tip of the mouth at the anterior end to the tip of the caudal fin at the posterior end. Figure 21 and Table 7 describe this landmark. As can be seen from Figure 21, there is a large variation in the dorsal length between all the lines analyzed. There are also significant differences in the southern lines themselves. Overall, the Icab is the longest and the Kaga the shortest at both 10 and 20 dpf. Interestingly, there is no significant difference ($p > 0.05$) between the HO5 and HNI lines at both time points.

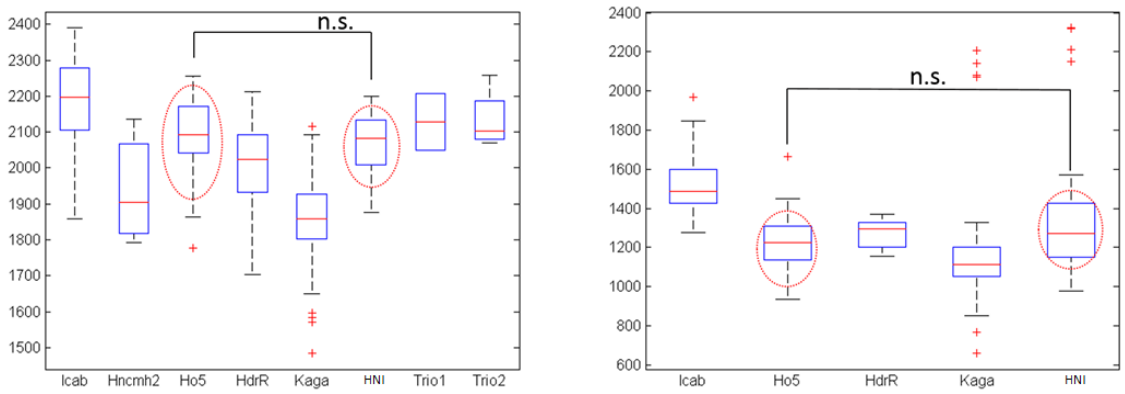

Figure 21 Dorsal length of the different lines. The y-axis is the length in pixels. (a). At10 dpf using at 20 x zoom factor. (b). At 20 dpf using a 10 x zoom factor. Significant differences in length are observed between the lines with Icab being the longest and the Kaga line being the shortest. No significant difference is observed between the representative lines: HO5 and HNI.

	Sample Size	Mean	Median	Standard Deviation
Icab	79	2181.738	2197.101	125.44
Hncmh2	16	1939.717	1904.9405	129.53
HO5	53	2087.4623	2092.138	118.77
HdrR	76	2006.764	2024.089	108.02
Kaga	122	1862.899	1857.5545	113.9
HNI	46	2067.788	2081.539	78.9597
Trio 1	2	2128.3655	2128.3655	112.48
Trio 2	4	2133.3685	2103.2275	85.0822

(a)

	Sample Size	Mean	Median	Standard Deviation
Icab	24	1.5290e+03	1.4866e+03	166.6860
HO5	25	1.2405e+03	1.2263e+03	157.4734
HdrR	16	1.2704e+03	1.2944e+03	74.2816
Kaga	48	1.1971e+03	1.1135e+03	338.8127
HNI	23	1.4135e+03	1.2745e+03	415.9160

(b)

Table 7 Dorsal length statistics. (a). At 10 dpf. (b). At 20 dpf.

Eye diameter normalized to the lateral length

The first lateral landmark quantified was the eye diameter. As seen in Figure 22 (and Table 8), the normalized eye diameter remains relatively constant between 10 and 20 dpf for the respective lines. There is also no significant difference between the eye diameter of the HO5 and HNI lines. However, there are significant differences among the southern and northern lines. The Icab individuals have the smallest diameter and the northern Kaga individuals showing the largest diameter when normalized to the lateral length. While the HdrR has a larger normalized eye diameter compared to the Icab individuals at 10 dpf, at 20 dpf there is no significant difference.

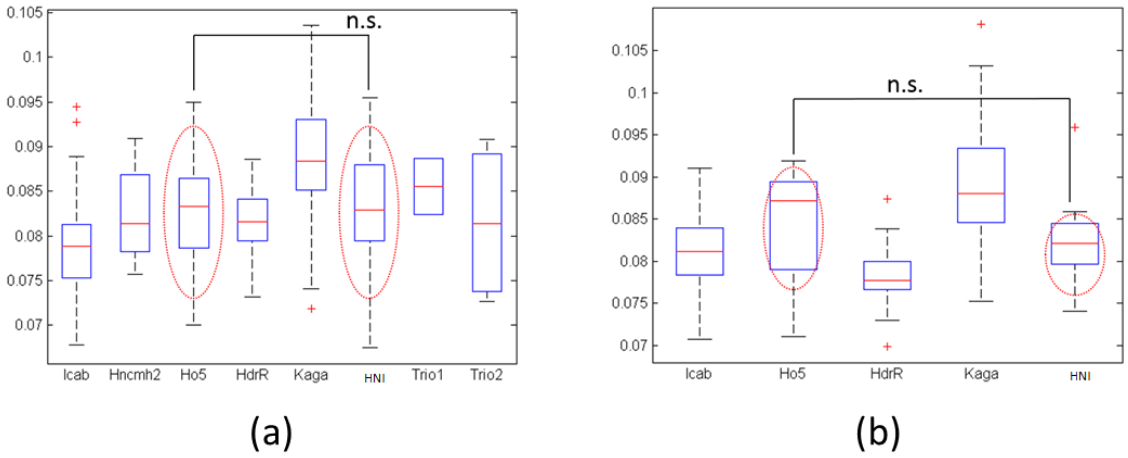

Figure 22 Eye diameter normalized to the lateral length. (a). At 10 dpf there are differences among the southern and northern individuals. (b). At 20 dpf. The eye diameter remains relatively constant between the two time points. There are no significant differences between the HO5 and HNI lines.

	Sample Size	Mean	Median	Standard Deviation
Icab	80	0.0785	0.0788	0.0051
Hncmh2	10	0.0824	0.0814	0.005
HO5	52	0.0827	0.0833	0.0054
HdrR	70	0.0815	0.0816	0.0035
Kaga	108	0.089	0.0883	0.006
HNI	41	0.0832	0.0829	0.0058
Trio 1	2	0.0856	0.0856	0.0044
Trio 2	4	0.0815	0.0813	0.009

(a)

	Sample Size	Mean	Median	Standard Deviation
Icab	24	0.0812	0.0811	0.0048
HO5	25	0.0845	0.0872	0.0060
HdrR	16	0.0782	0.0776	0.0040
Kaga	48	0.0889	0.0881	0.0069
HNI	23	0.0821	0.0821	0.0043

(b)

Table 8 Eye diameter normalized to the lateral length. (a). At 10 dpf. (b). At 20 dpf.

Lateral width before the beginning of the yolk sac normalized to lateral length

The first of the two lateral widths quantified is the width measured just before the beginning of the yolk sac (Fig. 16b). Figure 23 and Table 9 show the relevant measurements. Firstly, there is very significant difference between the HO5 and HNI lines both at 10 and 20 dpf. As before, at 10 dpf there is variation among the different southern lines with Icab and Hncmh2 being close to each other and HO5 and HdrR being close to each other. However, at 20 dpf differences start to show between HO5 and HdrR. For the northern lines studied, Kaga and HNI are both seen to be significantly different at both time points. Interestingly, at both time points, the southern HdrR and northern Kaga are close to each although significant differences are seen between HO5 and HNI.

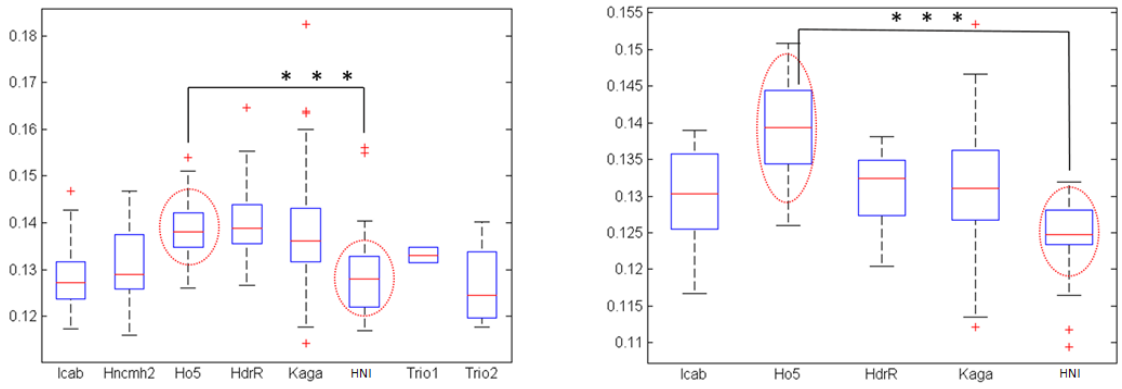

(a) (b)

Figure 23 Lateral width measured before the beginning of the yolk sac normalized to the lateral length. (a). At 10 dpf. Significant differences are observed among and between the different lines. The HO5 and HNI are very significantly different. (b). At 20 dpf. Very significant difference is still observed between HO5 and HNI. HdrR and HO5 which were quite similar at 10 dpf begin to show differences at 20 dpf.

	Sample Size	Mean	Median	Standard Deviation
Icab	80	0.1282	0.1272	0.0064
Hncmh2	10	0.1305	0.1289	0.0085
HO5	52	0.1382	0.1380	0.0063
HdrR	70	0.1398	0.1389	0.0066
Kaga	108	0.1381	0.1362	0.0101
HNI	41	0.1290	0.1279	0.0087
Trio 1	2	0.1331	0.1331	0.0023
Trio 2	4	0.1267	0.1245	0.0097

(a)

	Sample Size	Mean	Median	Standard Deviation
Icab	24	0.1301	0.1303	0.0062
HO5	25	0.1393	0.1393	0.0076
HdrR	16	0.1312	0.1325	0.0052
Kaga	48	0.1316	0.1310	0.0079
HNI	23	0.1243	0.1248	0.0057

(b)

Table 9 Lateral width measured before the beginning of the yolk sac normalized to the lateral length. (a). At 10 dpf. (b). At 20 dpf.

Lateral width normalized to the lateral length

The second width related morphometric distance in the lateral orientation is the width across the middle of the yolk sac (Fig. 16b). This width is of importance as it correlates to the size of the yolk sac. Figure 24 and Table 10 summarize the data for this parameter. At 10 dpf, there is very significant difference ($p <<< 0.001$) between the normalized lateral width of the HO5 and HNI lines. But, at 20 dpf this difference is not significant anymore ($p > 0.05$). The differences between the individual lines that are seen at 10 dpf tend to get smaller at 20 dpf.

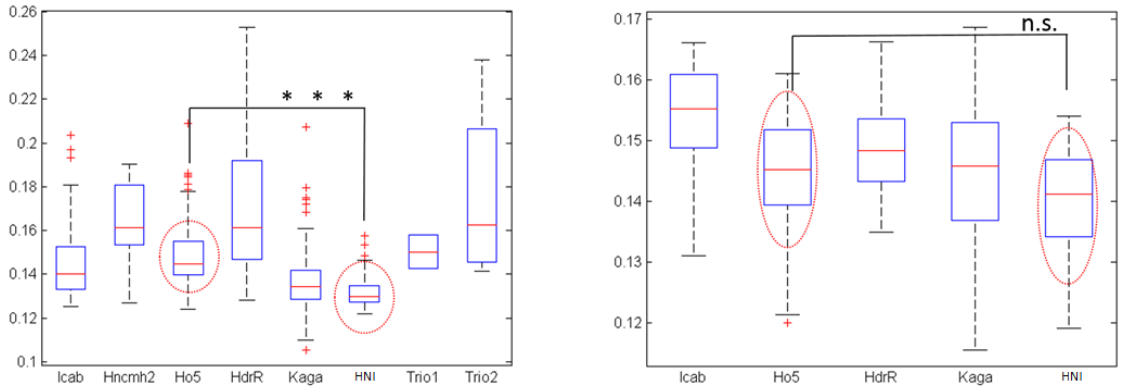

(a) (b)

Figure 24 Lateral width normalized to the lateral length. (a). At 10 dpf very significant differences are observed between HO5 and HNI lines. (b). At 20 dpf the differences HO5 and HNI are not significant.

	Sample Size	Mean	Median	Standard Deviation
Icab	80	0.1456	0.1401	0.0173
Hncmh2	10	0.164	0.1615	0.0196
HO5	52	0.1504	0.1447	0.0187
HdrR	70	0.1707	0.1613	0.0284
Kaga	108	0.1368	0.1343	0.0152
HNI	41	0.1321	0.1299	0.008
Trio 1	2	0.1502	0.1502	0.0109
Trio 2	4	0.176	0.1626	0.0436

(a)

	Sample Size	Mean	Median	Standard Deviation
Icab	24	0.1537	0.1553	0.0091
HO5	25	0.1443	0.1453	0.0110
HdrR	16	0.1495	0.1484	0.0085
Kaga	48	0.1444	0.1459	0.0122
HNI	23	0.1395	0.1412	0.0111

(b)

Table 10 Lateral width normalized to lateral length. (a). At 10 dpf. (b). At 20 dpf.

Lateral length

The last morphometric feature to be characterized for the inbred panel was the lateral length. It is the total distance from the tip of the mouth at the anterior end to the tip of the fin at the posterior end in the lateral orientation (Fig. 16b). As can be seen from Figure 25 and Table 11, at both time points there are variations in length among the southern and northern lines. Similar to the dorsal length, as would be expected, the Icab is longest and the Kaga individuals are the smallest in terms of length. There is no significant difference between the HO5 and HNI lines at both 10 dpf and 20 dpf ($p > 0.05$).

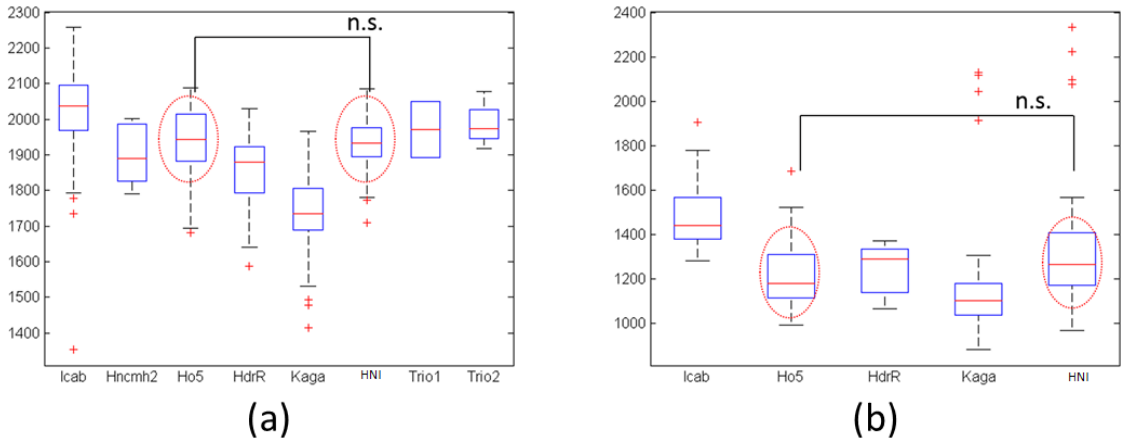

Figure 25 Lateral length. The y-axis is length in pixels. (a). At 10 dpf at 20 x zoom factor: No significant differences observed between HO5 and HNI lines. Differences are seen among southern and northern lines. (b). At 10 dpf at 10 x zoom factor: No significant difference between HO5 and HNI. Differences among southern and northern lines can still be observed.

	Sample Size	Mean	Median	Standard Deviation
Icab	80	2016.1089	2037.564	130.4475
Hncmh2	10	1899.7318	1889.266	85.4364
HO5	52	1937.9264	1944.1645	96.3895
HdrR	70	1854.7904	1878.9605	98.3455
Kaga	108	1740.6117	1736.255	105.8033
HNI	41	1930.1593	1933.214	75.0756
Trio 1	2	1972.013	1972.013	110.5887
Trio 2	4	1986.3055	1974.119	67.3167

(a)

	Sample Size	Mean	Median	Standard Deviation
Icab	24	1.4885e+03	1.4409e+03	157.9945
HO5	25	1.2277e+03	1.1790e+03	166.2848
HdrR	16	1.2499e+03	1.2931e+03	105.2443
Kaga	48	1.1920e+03	1.1034e+03	315.6714
HNI	23	1.3939e+03	1.2666e+03	397.6591

(b)

Table 11 Lateral length. (a). At 10 dpf. (b). At 20 dpf.

Summary of the morphometric analysis of the Medaka inbred lines

The first reassuring result was that the automated quantification of body length from both the dorsal and the lateral perspectives was almost perfectly correlated (Spivakov et al., 2014). Figure 26 shows the comparison between the mean lengths derived from the two viewpoints at both 10 and 20 dpf.

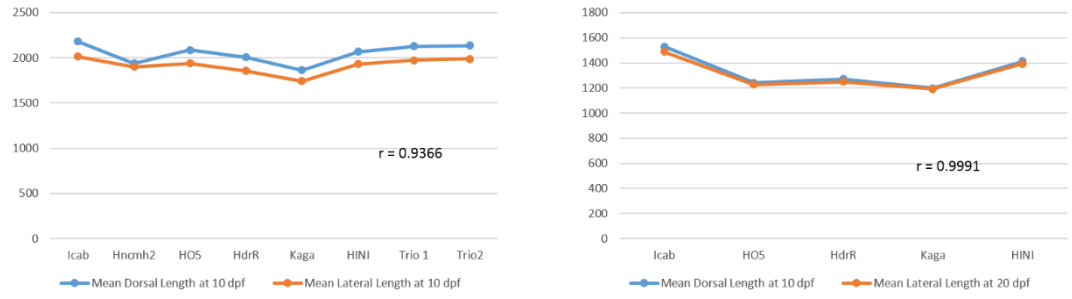

(a) (b)

Figure 26 Comparison of the total body length from dorsal and lateral orientations. (a). At 10 dpf the Pearson correlation coefficient is ~ 0.94. (b). At 20 dpf the correlation coefficient is ~ 1.

It is observed that the total body lengths of the HO5 and HNI lines were similar and showed no significant differences both at 10 and 20 dpf. This was one of the main reasons to choose these two lines as representatives of the southern and northern populations respectively. However, there is variation in body length “within” the different southern and northern populations. Since majority of the variance between individuals in a fish correlates with the body length, the morphometric features were all normalized to the body length (Spivakov et al., 2014).

Two morphometric parameters, the distance between the eyes (measured in the dorsal orientation) and the eye diameter (measured in the lateral orientation), are craniofacial features that play an important role in the vision system. Interestingly, given that the southern HO5 and the northern HNI lines have similar total body lengths they differ significantly in the distance between the eyes while the diameter of the eyes are similar.

Finally, from the prey capture mechanism perspective, there is a significant difference in lip width between the different lines and the difference becomes more pronounced at 20 dpf between the HO5 and HNI lines. Variations are also observed among the southern individuals for this feature at 20 dpf.

Behavior

Three behavioral patterns were characterized and compared across the different inbred lines and with zebrafish. The aim was to establish that differences exist in behavior among the inbred lines and to quantify these behavioral patterns and further populate the phenotype matrix. The behavioral phenotypes that were characterized are: spontaneous locomotion, feeding

behavior and finally prey capture behavior. All the behavioral assays were conducted with hatchlings at 10 dpf.

Spontaneous locomotion

Medaka begin to exhibit spontaneous locomotion just after hatching around 10 dpf. It was observed that different Medaka lines showed different locomotion behavior. In order to quantify this behavior, hatchlings from the southern HO5 and the northern HNI lines were used. As described in Figure 11, motion was recorded for each hatchling in 3 minute durations over 3 hours. The experiment was conducted at 3 different time points (as described in the experiment protocol in the Methods chapter) to account for time-of-day effects. Using the automated tracking algorithm, two parameters were quantified: the average distance travelled in 3 minutes and the speed of motion. Figure 27 shows the comparison of locomotion between the HO5 and HNI lines.

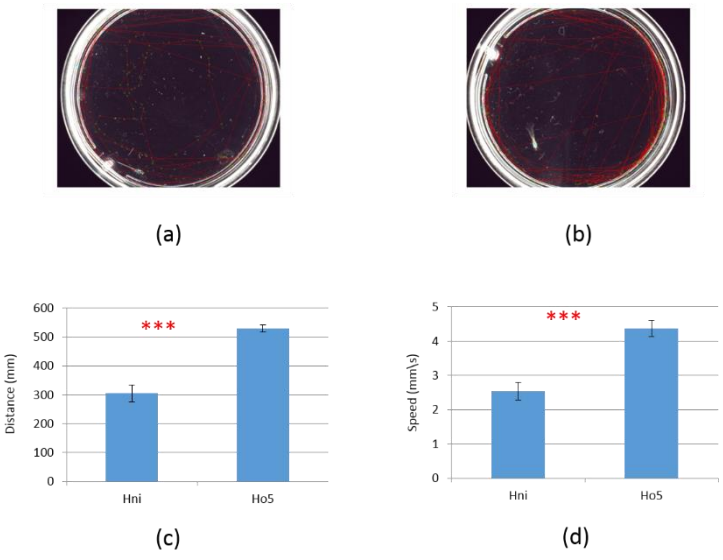

Figure 27 Comparison of locomotion behavior between HO5 and HNI lines. (a). Example of motion track for HNI. (b). Example of motion track for HO5. (c). Average distance travelled in 3 minutes. Very significant difference observed between HO5 and HNI. (d). Average speed of motion in the 3 minute window. Very significant difference observed between the two lines (P <<< 0.001).

Very significant differences are observed in both the distance travelled and the speed between the northern HNI and southern HO5 lines. While the HNI line was slower, the hatchlings explored the experimental arena much more. The HO5 hatchlings showed very rapid locomotion and mostly showed movement along the boundaries of the arena and occasionally moving into the center of the arena. Since, both lines exhibit anxiety when first introduced into the arena, only the data after acclimatization was used in the analysis.

Feeding behavior

A preliminary analysis of feeding rate among two southern lines (the Icab and the HdrR) was conducted to identify if any differences exist among hatchlings at 10 dpf with regard to the amount food consumed. Indeed, it was observed that there are differences not just between the lines but also among individuals drawn from the same line. The experiment performed was similar to the locomotion analysis but with about 100 paramecia provided to the hatchlings. The hatchlings were then recorded for about 10 hours after being given the paramecia. The amount of paramecia left in the petri-dish after each hour is then automatically analyzed according the algorithm described in Figure 13. Figure 28 shows the preliminary results.

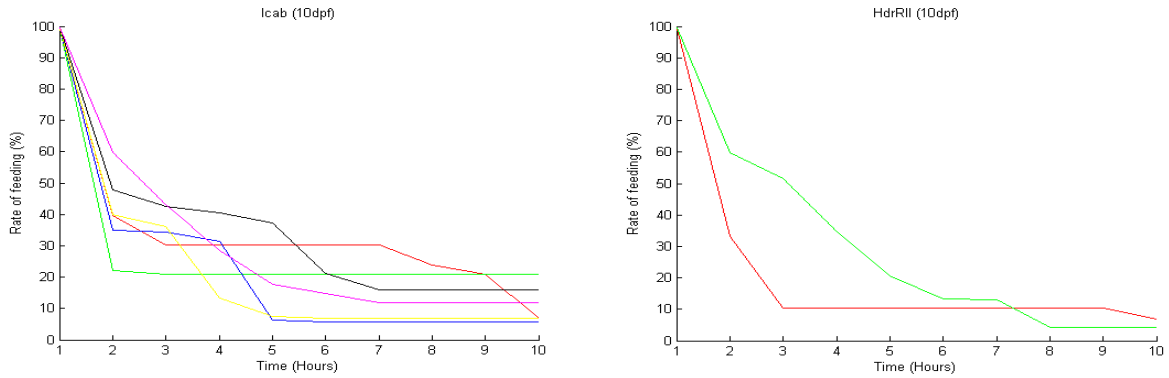

(a) (b)

Figure 28 Comparison of feeding rate between two southern lines. (a) Icab at 10 dpf. (b) HdrR at 10 dpf. While both lines consumed 90 % of the paramecia in about 5 – 6 hours, there are still significant individual differences.

It is observed from Fig. 28 that most of the individuals consumed about 60 % of the food within the first 2 hours. But, there are still very large variations in how the individuals fed. This was the motivation to understand prey capture mechanism in Medaka hatchlings and to also compare it with how the related organism, the zebrafish, captures prey.

Prey capture behavior

Prey capture is an innate goal-directed behavior responsible for feeding success and critical for ensuring the survival of an organism. This fundamental trait manifests itself very early in an organism's developmental process. The mechanism of prey capture involves the use of specific sensory modalities and the execution of certain movements drawn from an organism's repertoire of locomotion patterns. Different organisms exhibit different prey capture strategies depending on the environment and the nature of the prey. Studying prey capture, therefore, allows one to dissect sensory and motor system architecture in an organism. Larval/juvenile zebrafish have been used to study prey capture behavior to understand the complex locomotion strategies employed during this behavior (Borla et al., 2002; McElligott & O'Malley D, 2005). However, currently no prey capture studies have been performed on Medaka hatchlings.

The zebrafish use vision as the sensory modality in prey capture (Gahtan et al., 2005). To date, there is no report on sensory modalities employed by juvenile Medaka for prey capture behavior. Vision based goal-directed behavior starts with target identification followed by the execution of a series of movement patterns resulting in the capture of the target (Trivedi & Bollmann, 2013). The movements themselves could be discrete or continuous in time with the aim of resolving target coordinates and trajectory and using visual feedback to finally achieve the intended goal (Land, 1992b).

Prey capture behavior starts to manifest itself in zebrafish around 5 days post fertilization (dpf) while Medaka demonstrate it from 10 dpf (just after dechorionation). At these developmental time points, the zebrafish and the Medaka have similar size attributes (being about 4 mm in length). Previous studies have identified the zebrafish locomotion repertoire (Fero et al., 2011).

Types of locomotion patterns in Medaka during prey capture

Several studies have been reported to understand axial kinematics and visually guided prey capture behavior in zebrafish (Bianco et al., 2011; Borla et al., 2002; Fero et al., 2011; McElligott & O'Malley D, 2005; Trivedi & Bollmann, 2013). We begin with trying to find the locomotion patterns in Medaka during prey capture.

When free swimming Medaka are provided with paramecia in a small petri-dish, they execute different locomotion patterns and capture the paramecia. Using the high-speed imaging system described in Figure 14 (Trivedi & Bollmann, 2013) 18 independent prey capture episodes of the HNI strain and 9 episodes of the HO5 strain were recorded. Each episode consists of one hatchling capturing a single paramecium. An analysis of all these video sequences revealed four consistent locomotion patterns exhibited by both strains of Medaka during the prey-capture event. Figure 29 shows an example prey-capture sequence that reveals these patterns. The first was the large rostro-caudal asymmetrical bend that facilitates large turns and is also seen to contribute to the first significant movement towards the prey. The second pattern observed were small symmetrical tail movements that were used for facilitating forward movement and slow swimming. Small asymmetrical caudal tail bends constituted the third set of patterns to provide small angular adjustments and was employed just before the final capture event. Finally, a rapid short-duration turn of the head, referred to as the “head snap”, with the

body exhibiting a characteristic bending to assist the snap was used to consume the prey.

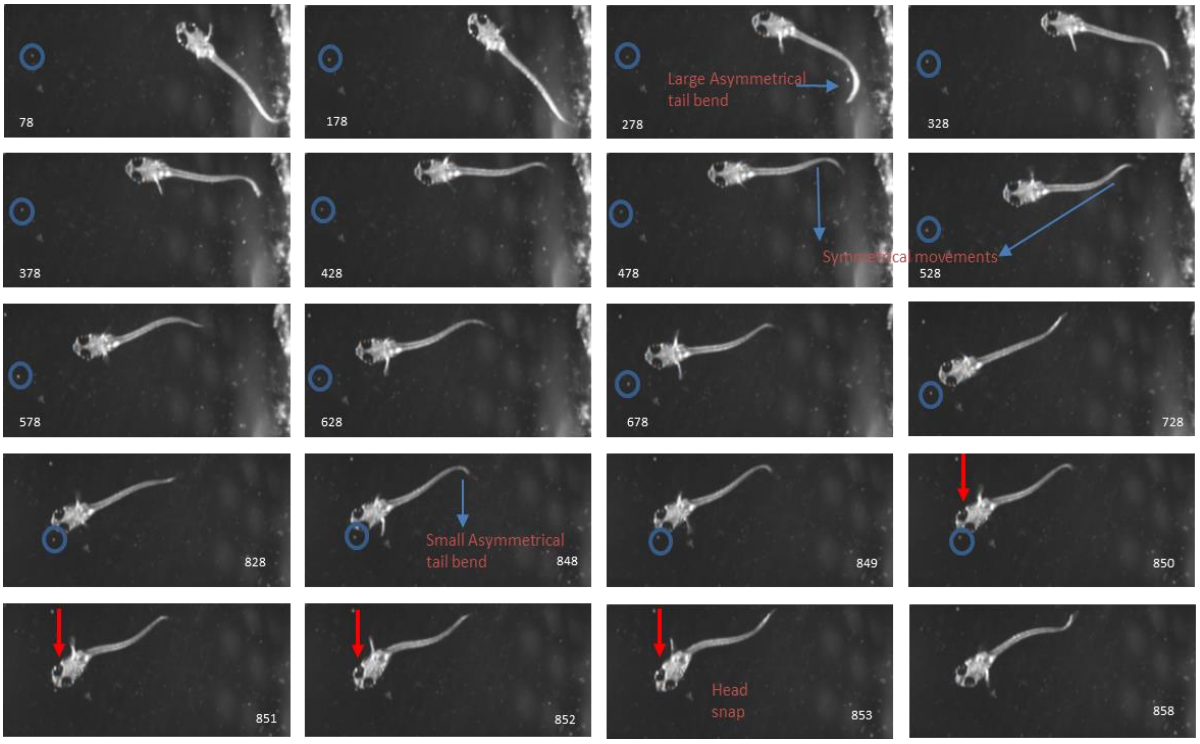

Figure 29 Locomotion patterns exhibited by Medaka during an episode of prey capture. The blue arrows show the large asymmetrical tail bend (used to execute a large angle turn and is the first movement towards the prey: the initiation phase, the symmetrical tail bends used for slow swimming and forward movements: the swim phase; small asymmetrical tail bends to make small adjustments before the prey capture: the pre-snap phase. The red arrows show the short "head snap" movement used to consume the prey: the snap phase. The blue circle shows the position of the paramecium.

Based on these locomotion patterns we divide an entire Medaka prey-capture episode into four phases. The first phase is the 'initiation' phase where the Medaka detect the presence of the prey and perform the first large movement towards the prey. The second phase, which we call the 'swim' phase, is characterized by the fish moving towards the prey and is temporally chosen to be half-way between the initiation phase and the end of the third phase called the 'pre-snap' phase. The pre-snap phase occurs just before the final capture event and involves the culmination of minor angular adjustments and the start of the final phase. The final phase is the 'snap' phase which constitutes the head snap to consume the prey.

Prey tracking and capture in Medaka

For prey capture, larval zebrafish perform a series of approaching maneuvers which are interrupted by brief pauses. The sequence terminates with a capture swim when the prey is at striking distance. So, zebrafish exhibit a discrete or intermittent prey capture behavior which involves swimming bouts interspersed with pauses (Kramer, 2001; McElligott & O'Malley D, 2005). Furthermore, it was shown that the individual swimming bouts are an elementary motor pattern which is superimposed with a graded turning component controlled by visual feedback to form a goal-directed motor sequence (Trivedi & Bollmann, 2013). Importantly, it was observed that the zebrafish detect the target preferably monocularly while the subsequent tracking and capture phases are binocular (Bianco et al., 2011; Patterson et al., 2013; Trivedi & Bollmann, 2013). Quantitative analysis of larval zebrafish prey capture from (Trivedi & Bollmann, 2013) determined the midline of the larva in each frame of the high-speed videos and computed the angular deviations, γ_1 – γ_5 of five tail segments from the body axis. Furthermore, the angle between the prey position and the body axis (φ), the prey distance with respect to the midpoint between the eyes (d) and the orientation of the fish (Θ) were extracted. This parametrized the prey capture sequence using a set of 8 observables ($\gamma_1 - \gamma_5$, d, φ, Θ). This is shown schematically in Fig. 15. Using the same approach, Medaka prey capture sequences were quantified in order to facilitate a comparison. Figure 30a – 30d show representative comparisons for the tail angle γ_5, the fish-prey angle φ, the orientation Θ and the fish-prey distance d between Medaka and zebrafish larva during one prey capture sequence.

The most important feature of the Medaka prey capture was that it was executed in continuous motion (Fig. 30a). There were no pauses or individual

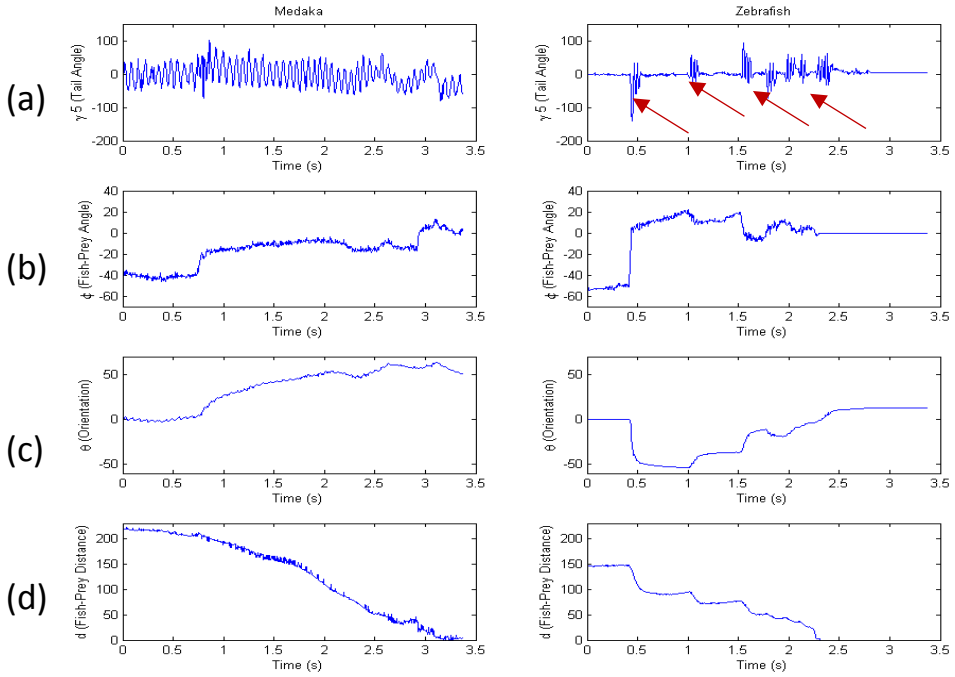

Figure 30 Comparison of prey capture parameters between Medaka (left panel) and zebrafish (right panel). (a). Tail angle γ_5 showing that Medaka have a continuous motion during prey capture as opposed to zebrafish that has discrete intermittent motion (red arrows). (b) Fish-prey angle in both Medaka and zebrafish reduces with time but in Medaka it is more continuous. (c)Orientation. Zebrafish orient towards the prey at the beginning of the prey capture sequence while Medaka do not orient themselves completely in the line-of-sight of the prey. (d). Distance to prey reduces monotonically in both but again with differences in the continuous and discrete approach.

swimming bouts but rather a continuous movement towards the prey. This is in sharp contrast to the zebrafish behavior which employs discrete swimming bouts interspersed with pauses.

Figure 30b shows that the fish-prey angle in both the Medaka and the zebrafish reduces with time. However, while in zebrafish the first few bouts bring it almost in the line-of-sight of the prey, in Medaka the reduction in the angle is more continuous and decreases over time. The orientation of the fish with respect to the prey over time can be seen in Fig. 30c. The zebrafish orient themselves to be aligned to the prey directly in the beginning of the prey capture sequence while the Medaka never orient themselves such that they are

directly aligned to the prey, always tending to keep the prey to one side of their midline (Fig. 39b). Finally, Fig. 30d shows that both Medaka and zebrafish monotonically reduce the distance to the prey over time. However, the zebrafish does this in discrete steps while the Medaka reduces the distance continuously over time.

As discussed above, and to reiterate, since the Medaka prey capture event does not have individual swim bouts, the prey capture episode is divided into four phases (Fig. 29): 1. the initiation phase, 2. the swim phase, 3. the pre-snap phase and finally 4. the snap phase.

The mean distances to the prey for all the capture sequences both for the HNI and HO5 lines were compute and are shown in Fig. 31.

(a)

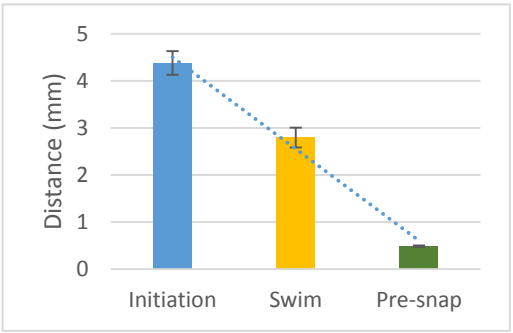

(b)

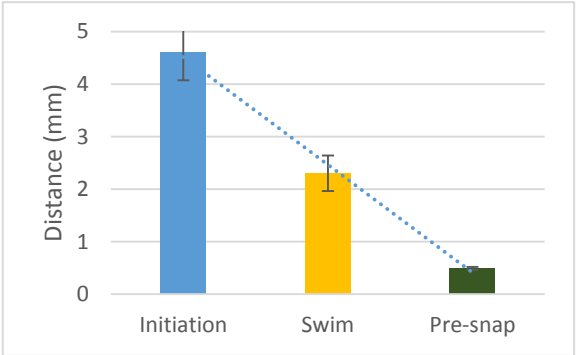

Figure 31 Comparison of mean distances to the prey for the two lines: HNI shown in (a) and HO5 shown in (b). There is a monotonic decrease in distance to the prey over the different phases. The distance to the prey just before the snap phase is identical for both lines.

The mean distances to the prey in the initiation phase for HNI was 4.37 ± 0.25 mm and for the HO5 line it was 4.6 ± 0.53 mm. In the swim phase, for the HNI the distance was 2.79 ± 0.21 mm and 2.3 ± 0.33 mm for the HO5 line. Finally, in the pre-snap phase just before the final capture event, the mean distance to the prey for the HNI line was 0.49 ± 0.01 mm and 0.49 ± 0.03 mm for the HO5 line. As can also be seen from Fig. 31, the trend lines confirm that there is a monotonic decrease in distance between the fish and the prey over the 3 phases of prey capture. Finally, the distance to the prey just before the final capture event is identical in both lines.

In order to systematically investigate vision directed Medaka prey capture, three types of eye angles were computed for all the sequences: 1. The angle the prey makes with the midline (body axis) of the fish; 2. The ipsilateral and contralateral eye angles with respect to the body axis and 3. The ipsi- and contralateral eye angles with respect to the prey as well. An illustration of the different eye angles is given in Fig 32.

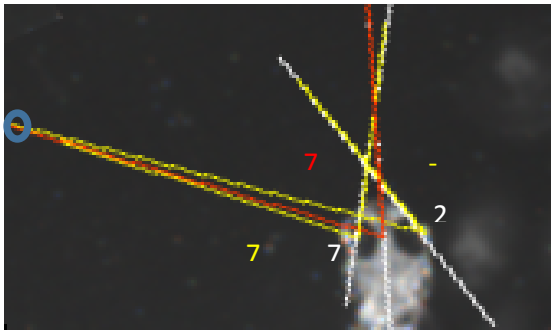

Figure 32 Eye angles computed to understand vision directed prey capture in Medaka hatchlings. The blue circle denotes the location of the prey. Red: the angle the prey makes with respect to the body axis. White: the ipsi- and contralateral eye angles. Yellow: The angle the prey makes on the ipsi- and contralateral eyes.

Depending on whether the prey was visible to the ipsilateral or the contralateral eye in the initiation phase, the angle the prey made to the body axis (shown in red in Fig. 32) was computed for all sequences. This distribution is shown in Fig. 33.

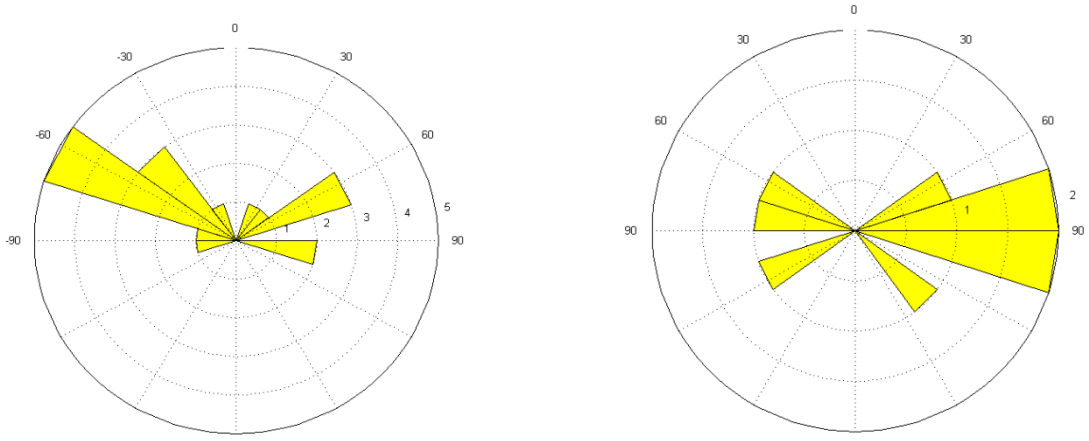

(a) (b)

Figure 33 Distribution of the angle of the prey in the initiation phase. Mean angle when prey capture was initiated was (mean ± s.e.m.): (a). HNI: 64.5° ± 5.03°. (b). HO5: 91.33° ± 7.86°.

It is observed that the prey was preferentially detected at the initiation phase for HNI only at angles greater than 32° (the mean being 64.5° ± 5.03°, 32° < φ < 104°) and with the prey being invisible to the contralateral eye. For the HO5 strain, the detection happens at angles greater than 61° (the mean being 91.33° ± 7.86°, 61° < φ < 140°). Clearly, the HO5 line individuals have a larger angle with respect to the prey before initiation as compared to the HNI line. Since the prey was completely invisible to the contralateral eye at initiation, it can be

concluded that prey capture in Medaka is initiated monocularly. This was reported to be similar in zebrafish (Trivedi & Bollmann, 2013).

However, the intriguing feature of the prey capture sequences in Medaka was that the orientation of the fish was never aligned to that of the prey and the Medaka tended to position themselves in such a way as to keep the prey always lateral to their body axis. This suggested strongly that the Medaka prey capture maybe completely monocular (as opposed to the zebrafish which changes to binocular prey capture locomotion after monocular detection).

Monocular prey capture in Medaka hatchlings

We begin with evaluating the position of the prey with respect to the ipsi- and contralateral eye angles (shown in white in Fig. 32) in the first three temporal phases of prey capture: the initiation point, the swim point and the point just before the head snap movement for capture occurs. An illustration of this is given in Fig. 34.

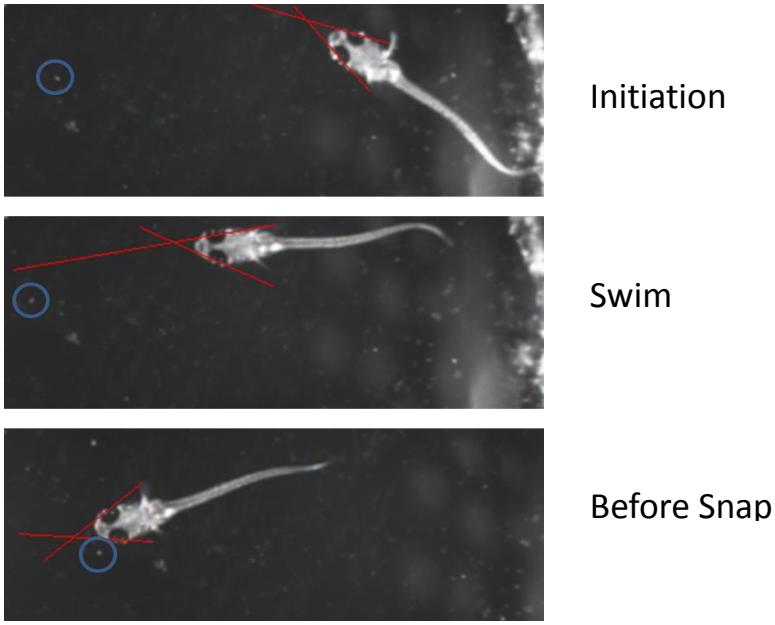

Figure 34 The position of the prey (indicated with the blue circle) with respect to the ipsilateral and contralateral eye angles at three temporal points during prey capture. As is observed in all the three phases, the prey is never in the binocular field-of-view of the fish suggesting that prey capture in Medaka hatchlings is monocular.

As can be seen from the three temporal snapshots of a typical prey-capture sequence in Fig. 34, in none of the time points, during the progression of the prey-capture event, does the prey ever come into the binocular field-of-view of the fish's vision. The prey is always invisible to the contralateral eye. In fact, it was observed in the prey capture sequences that the hatchlings made an effort to always keep the prey on one side of the body axis. This strongly suggests that Medaka seem to prefer monocular prey tracking and capture. To obtain a quantitative evidence of this, we also quantified ocular vergence angles at the three different time points as shown in Fig. 35.

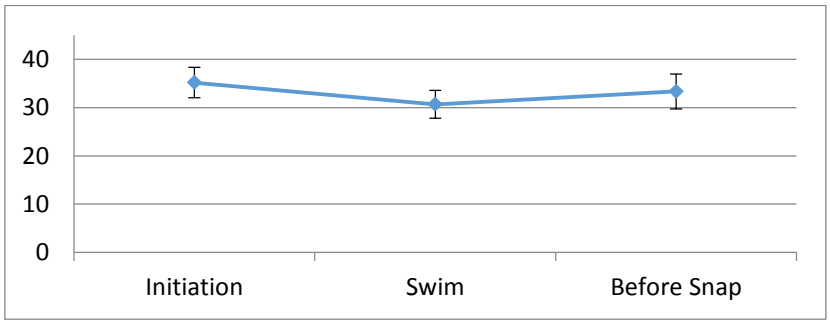

(a)

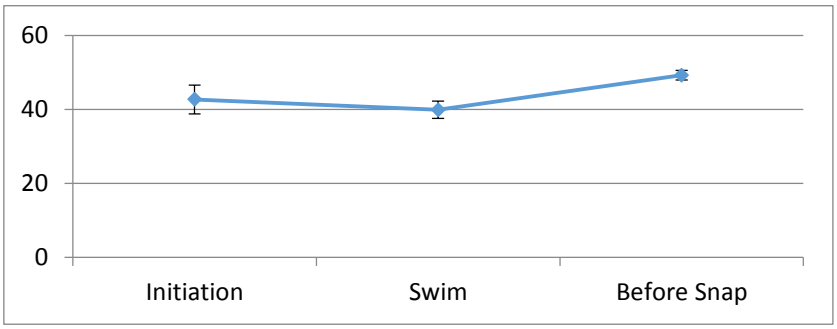

(b)

Figure 35 Ocular vergence angles (mean ± s.e.m) at the initiation point, swim point and before snap point for HNI and HO5 lines shown in (a) and (b) respectively. There is no significant change in vergence during the prey capture sequence.

The vergence angles at initiation for HNI and HO5 strains were: 35.1667° ± 3.1501° and 42.6667° ± 3.8586° respectively; at the swim point were: 30.6667° ± 2.8924° and 39.8889° ± 2.3596° respectively and at the pre-snap point were: 33.3333° ± 3.5874° and 49.2222° ± 1.31° respectively. There was no significant increase in the vergence angle in both the HNI and the HO5 lines between prey-capture initiation and the swim point ($p > 0.3$ for HNI and $p > 0.5$ for HO5, t - test) and between the initiation point and before snap ($p > 0.7$ for HNI and $p > 0.1$ for HO5, t – test). This is in sharp distinction to the zebrafish behavior where the ocular vergence increases substantially from the pre-capture to the strike phase where an increase vergence of close to 40° has been reported (Bianco et al., 2011). While there was no significant difference in vergence between the swim point and the before snap point in HNI individuals ($p > 0.3$, t-test), there was a slight significance in HO5 individuals ($p \sim 0.02$). We believe this is because of the limited number of HO5 prey capture episodes (N = 9) one outlier in the data. With this one outlier removed there was no significant difference anymore ($p \sim 0.08$). However, a more number of prey capture episodes for HO5 need to be analyzed.

To further investigate the monocular prey capture behavior, we studied the relation between the fish-prey angle and the angle the prey makes on the ipsi- and contralateral eyes for all the sequences at the three different time points. The eye angle is scored positive if the prey is visible to that eye and negative if it is not. Figure 36 shows the diagrammatic representation of this analysis for all the different phases. As can be seen, the eyes never position themselves in a way that the prey is visible to both eyes in both the HNI and HO5 lines. This gives further evidence that the prey capture mechanism is indeed monocular.

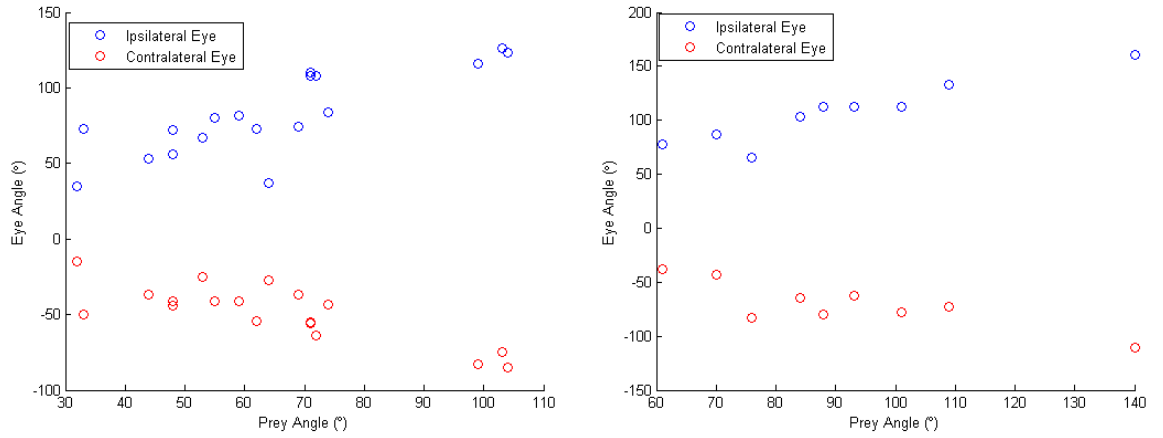

(a)

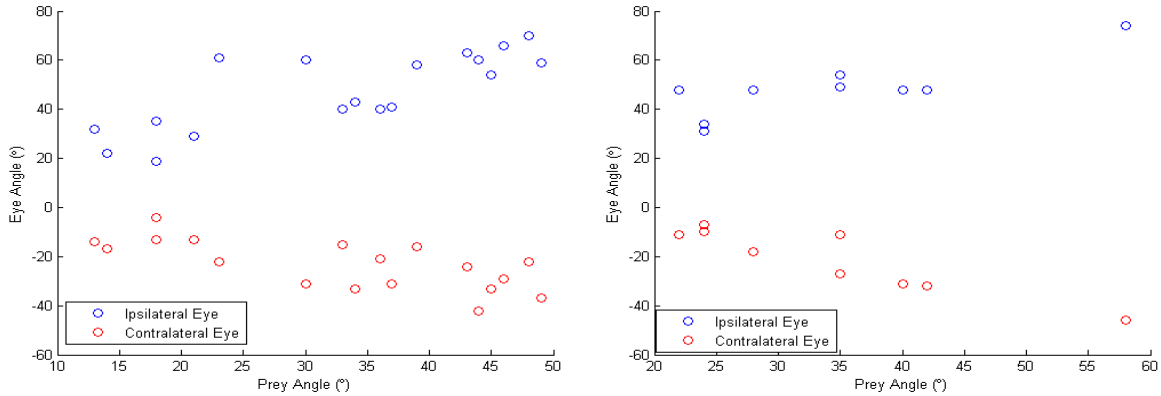

(b)

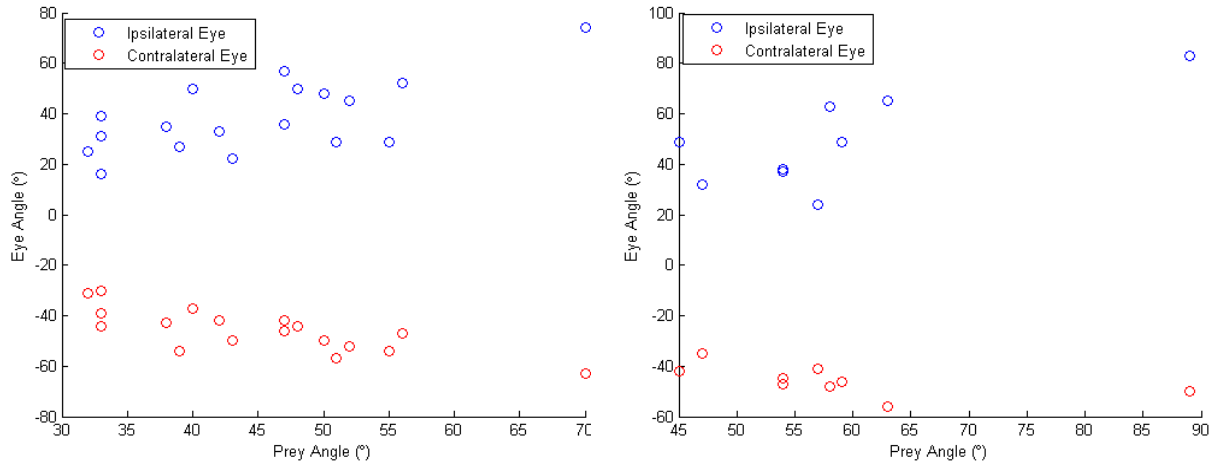

(c)

Figure 36 Comparison of fish-prey angle and the angle the prey makes on the ipsi- and contralateral eyes. The left panels is for the HNI line and right pane for the HO5 line. (a), (b), and (c) indicate the three different prey capture phases respectively. In none of the sequences, the two eyes are positioned such that the prey is visible to both eyes and thereby indicating monocular vision during prey capture.

Having qualitatively and quantitatively established the monocular prey capture behavior in Medaka, we investigated if there is a correlation between the initial prey angle and the change the fish makes in its orientation from the initiation point to the swim point. This is shown in Fig. 37. We computed the coefficient of determination that indicated a linear relationship between the two parameters.

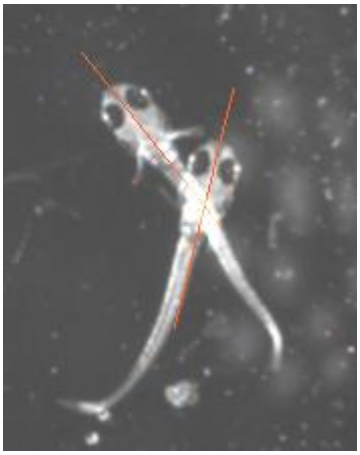

(a)

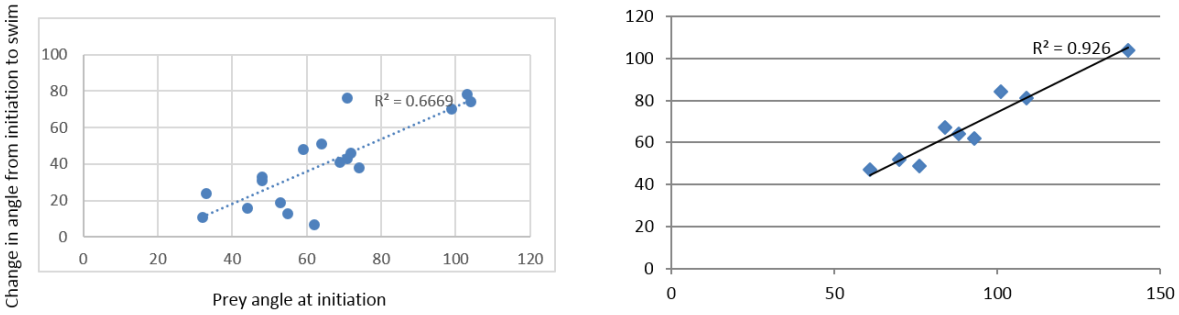

(b)

Figure 37 Prey angle vs. change in orientation of the fish from initiation to the swim point. (a). Illustration of the calculated angle. (b). HNI on the left side and HO5 on the right side show linear relation between the two.

One of the characteristic features in Medaka prey capture is the snap movement of the head to consume the prey. Figure 38a shows an overlay of

two time points: the before snap time point and the end of the snap movement time point. During the snap movement, the body of the fish exhibits a characteristic bending followed by a very short snap of the head (lasting between 28 – 32 ms on the average) to consume the prey. We quantified the angle of the snap movement and found the snap angle to be 26.67° ± 1.79° (mean ± s.e.m.) for HNI and 32.44° ± 2.8° for the HO5 strain. Furthermore, there was a correlation between the prey angle before snap and the angle of the snap itself, Fig. 38b, indicating that the snap angle depends on the angle the prey makes to the ipsilateral eye just before capture.

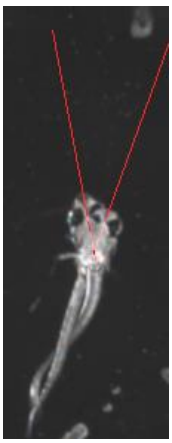

(a)

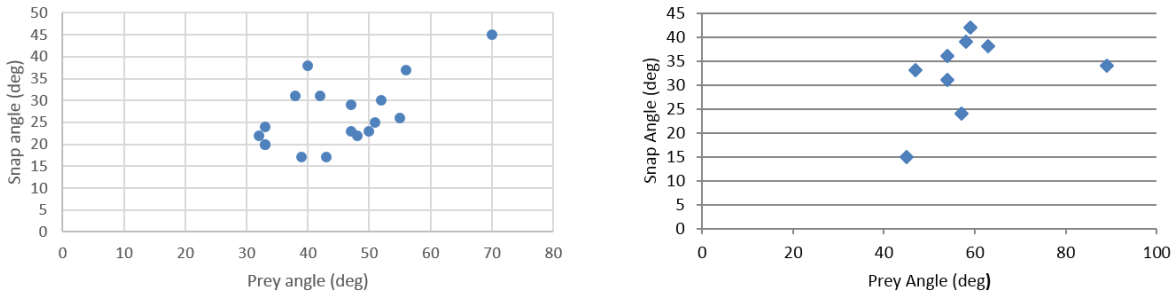

(b)

Figure 38 Head snap movement is a characteristic feature of prey capture in Medaka hatchlings. (a) An illustration of the movement of the head from before snap phase to the snap and capture phase. (b) Correlation between prey angle before snap and the angle after the snap is linear (Pearson's coefficient > 0.6).

Frequency analysis

We performed two frequency analyses to identify the frequency components in the locomotion patterns exhibited during the prey capture. Firstly, we computed the power spectral density of the temporal tail angle data. A representative spectrum is shown in Fig. 39a. We identified two major frequency components: one is the low frequency 3 – 5 Hz component and the other is the 15 – 20 Hz high frequency. We compared this with the zebrafish analysis from (Trivedi & Bollmann, 2013) and found that the zebrafish has a low frequency tail-angle component in the range of 3 – 5 Hz and a high-frequency component in the range of 20 – 35 Hz. We performed a time-frequency spectral decomposition and compared it with the temporal progression of the fish during a capture event (shown in Fig. 39b). We found that the high-frequency 15 – 20 Hz component corresponds to forward swimming with symmetrical tail beat motion. The low frequency 3 – 5 Hz component corresponded to angular changes in orientation of the fish.

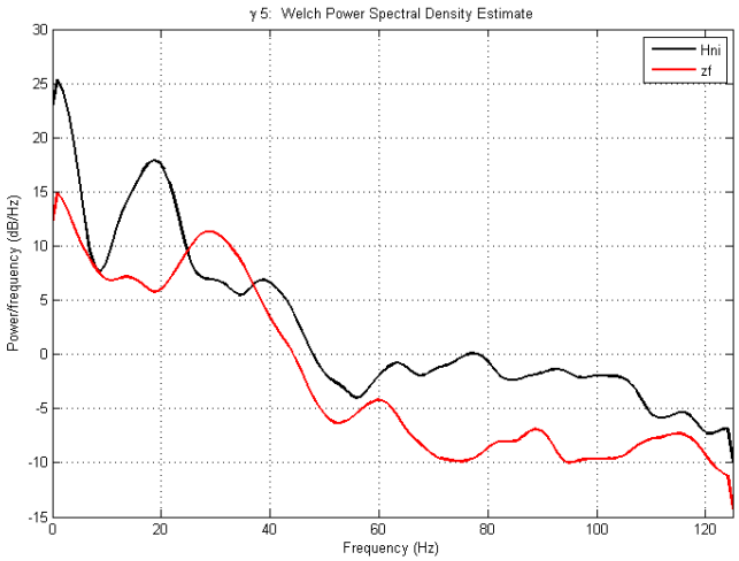

(a)

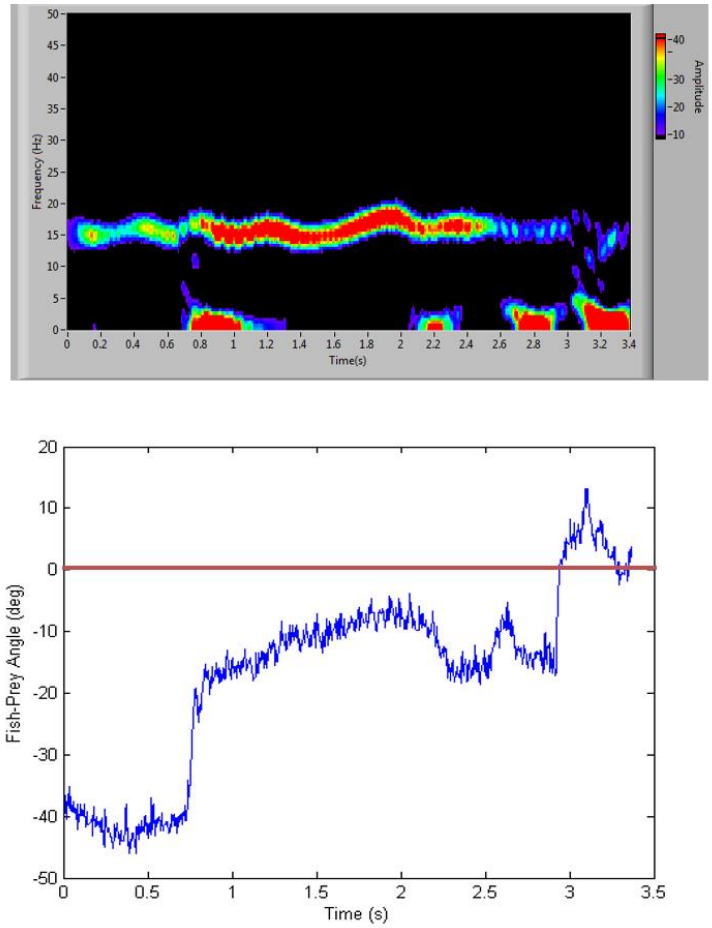

(b)

Figure 39 Frequency analysis of the tail beat. (a) Power spectral density analysis revealed a low frequency component between 3 – 5 Hz and and high frequency component of 15 – 20 Hz for HNI individuals. This is in contrast to zebrafish which shows a 3 – 5 Hz low frequency component and a 30 Hz high frequency component. (b) Spectrogram analysis revealed that the high frequency component corresponds to forward swimming with symmetrical tail movement and the low frequency component corresponds to angular changes when compared with the temporal progress of the hatchling. The red line indicates 0° suggesting that the Medaka do not orient themselves to the prey but rather approach it continuously.

Discussion and Outlook

Medaka are highly polymorphic organisms that show several phenotypic differences depending on their geographic origins. They are tolerant to inbreeding (Kirchmaier et al., 2015) and, therefore, provide a rich resource for genomic and phenotypic studies (Spivakov et al., 2014). Owing to their phenotypic variance they are ideal vertebrate model organisms that can be used to understand the relationship between the genotype, the environment and the phenotype (the G-E-P map) and for Genome Wide Association Studies to assess individual risk factors for disease and disorders.

The goal of this thesis was twofold: one was to establish a comprehensive phenotyping platform that can automatically image and analyze a number of phenotypic features of teleostei like Medaka and zebrafish and the second was to identify and quantify morphometric and behavioral phenotypes in juvenile Medaka using a panel of near-isogenic lines. The intention is to be able to establish a benchmark to form a comprehensive phenotypic matrix for the panel of approximately 200 inbred Medaka lines that is being set up.

Why study differences (with Medaka)?

Indeed differences hold populations together! (Reznick & Travis, 2017). Differences between individuals of a species and those between related species offer a way of understanding population structure, evolutionary mechanisms and adaptation to particular environments. It was shown in (Reznick & Travis, 2017) that stickleback fish living in lakes and streams differed substantially from each other in body shape and is the result of adaptive evolution determining the body shape best suited to the environment. However, frequency-

dependent selection favors rarity and therefore helps in maintaining genetic variations in a population (Reznick & Travis, 2017).

Medaka is ideal for studying differences as Medaka from different geographical locations show differences in size, color, form and behavior. Consequently, they can be used to study population variations due to latitudinal clines and biodiversity in general. Furthermore, this has translational relevance as humans have a significant variability across geographical regions with individuals from certain regions having a propensity to certain diseases to which individuals from other regions are not so susceptible.

In this thesis, the focus was on extracting and comparing differences in gross morphological features and a few behavioral patterns from Medaka hatchlings using a representative set of inbred lines.

Morphometrics

Morphology is a very useful trait to understand intraspecific variations and interspecific divergence. In Medaka, while adult craniofacial morphology has been studied (Kimura et al., 2007), no literature to our knowledge exists for hatchlings and for characterization of gross morphological features. In this work, four southern lines (Icab, HncmH2, HdrR and HO5), 2 northern lines (HNI and Kaga) and 2 trios were used to characterize dorsal and lateral landmarks in hatchlings at two developmental time points: 10 dpf and 20 dpf. All morphometric distances were normalized to the body length.

The dorsal lip width was significantly different among different individuals and especially different between the southern HO5 and the northern HNI lines (with HO5 having wider lip widths). The differences get more pronounced at 20 dpf. This is probably related to the nature of the food in the individual habitats

that require a different mouth construction to facilitate the ingestion of the prey. A similar significant difference was observed in the distance between the eyes with HO5 individuals tending to have a larger distance compared to the HNI individual. However, there were also differences among the southern and northern individuals. The dorsal width of the hatchlings were seen to be different for the HO5 and HNI lines at both time points. From the lateral perspective, the eye diameter was not significantly different among the lines. The lateral width measured across the middle of the yolk sac showed significant differences at 10 dpf but disappears at 20 dpf. For the HO5 and HNI lines the body lengths were not significantly different.

One conjecture to explain the differences between the HO5 and HNI could be the geographic separation between the southern and northern lines. It is also possible that there is ecological speciation owing to the different environments and the northern lines are a species of their own.

Outlook

While it is known that the individual habitats of HO5 and HNI are different, it will be interesting to study the habitats of the individual southern and northern lines to understand if there are any local differences. This could potentially explain differences among the southern and northern lines. Furthermore, in this study only two developmental time points were used. It is essential to correlate the morphometric features at these time points to other time points to see if which of these variations are preserved even in young and adult fish. Finally, are there other features and landmarks where the differences between the strains are significant? This is important to assess both for QTL mapping and for GWAS.

Behavior

Behavioral patterns are highly connected to the genome and are significantly influenced by the environment. So, understanding behavioral traits could reveal how organisms react to stimuli in their habitats and in dissecting their neural mechanisms. Locomotion and feeding are two fundamental and complex traits that are responsible for an organism's survival. In this thesis, for the first time, we present a qualitative and quantitative description of juvenile Medaka prey capture behavior.

The motivation for the study came from observations that showed differences in the spontaneous locomotion among the southern and northern lines. So, the HO5 and the HNI strains at 10 dpf were then extensively analyzed using the developed automated imaging platform and the associated algorithms. It was observed that while the HO5 individuals move faster and cover a larger distance on the average, they tend to move along the boundaries of the experimental arena and move into the center of the arena occasionally. This was in contrast with HNI individuals that moved slower, covered a shorter distance on the average but were more explorative. Furthermore, there were differences in the feeding rates among the different individuals. This suggests that probably the habitat plays a crucial role in determining exploratory and spontaneous locomotion while hunting for prey.

In order to understand the prey capture behavior in detail we systematically characterized hatchlings from the HNI and HO5 lines capturing a single paramecium using high speed video recordings. Firstly, we have empirical evidence that juvenile Medaka use vision as the sensory modality for prey capture. Our different high-speed video recordings of prey capture show Medaka can successfully find, track and prey on paramecia in a given arena using vision. We identify different locomotion patterns exhibited by Medaka

during prey capture and show that the Medaka track and capture the prey by continuous locomotion. Furthermore, we show that the Medaka execute the entire prey capture routine monocularly and employ a unique snap movement of the head to consume the prey. Finally, we perform spectral analysis to identify the spectral components in the locomotion patterns and to identify the functionalities of the different patterns. We compare Medaka prey capture behavior with the behavior zebrafish. The intent is to show how Medaka reveals interspecific variability and how two related species adopt strikingly different strategies in performing a similar and vital task necessary for survival.

Locomotion during prey capture

Observation and quantitative analysis of several video recordings of the predation, four distinct locomotion patterns could be identified. The Medaka perform large rostro-caudal asymmetrical bends in order to execute large angular turns. Since the prey was preferentially detected at angles greater than 32°, it was observed that this locomotion pattern was the first significant movement that propels the fish towards the prey after the initiation of the prey capture event. The fish execute small symmetrical tail movements for forward motion and slow swimming. This is seen during the prey capture swim after initiation. Small positional adjustments were seen to be made by using asymmetrical caudal tail bends. These bends were typically used just before the final capture event in order, possibly, to bring the fish to the right striking distance from the prey. All the three locomotion patterns described above are also seen in the zebrafish. However, the most unique locomotion pattern occurs in the final capture event. The Medaka execute a snap movement of the head, where the head snaps in the direction of the prey with a mean angle of about 26.67° and consumes the prey. During the snap movement, the whole body exhibits a bending which we believe facilitates the sharp movement of the

head. In comparison, the larval zebrafish employ two strategies in the final capture phase. One is the ram capture where the prey is consumed following forward movements and the other is the suction capture where the prey is consumed with almost no body movements. As explained in the Introduction chapter, the two feeding mechanisms are at the ends of a feeding continuum (Norton & Brainerd, 1993; Wainwright, 1999). In the case of Medaka, this final strategy of head snap is consistent across all the recordings suggesting that craniofacial morphology directs the hatchlings to thrust the mouth on to the prey and allows for the jaws to grasp the prey. Another hypothesis is probably the nature of the prey (in terms of size and movement) in the natural environment is such that normal suction does not work and the hatchlings overcome this by striking at the prey. In all the cases, the fish-prey angle before the snap movement showed very little variation. This could suggest a vision-based explanation which will be discuss later.

Another striking difference between zebrafish and Medaka predation events is that, while both decrease the distance to the prey monotonically, they differ in the nature of the locomotion. Larval zebrafish approach the prey in a series of swim bouts that are interrupted by brief pauses. Consequently, the entire prey capture event is discrete in time. However, the juvenile Medaka execute the prey capture in continuous motion. There are no pauses and the fish is constantly swimming towards the prey. So, in the absence of discrete swim bouts, we have created a nomenclature to identify different temporal events during prey capture in juvenile Medaka. We divide the capture episode into the ‘initiation’ phase, the ‘swim’ phase, the ‘pre-snap’ phase and finally the ‘snap’ phase.

Monocular vs. binocular prey capture

It was observed that the juvenile Medaka, in the initiation phase, preferentially detect the prey at angles greater than 32° among HNI individuals (mean 64.5° ± 5.03°) and at angles greater than 61° (mean 91.33° ± 7.86°) among HO5 individuals. Furthermore, the prey was always visible to only one eye, the ipsilateral eye, while being invisible to the contralateral eye. This clearly indicated that prey capture initiation in juvenile Medaka was monocular. A similar observation was also made in larval zebrafish prey detection (Trivedi & Bollmann, 2013). After detection, larval zebrafish orient themselves to be aligned with the prey almost immediately and thereby reducing the fish-prey angle to ~0° (Fig. 30b). From here onwards, the prey is always maintained in the binocular vision region until the final capture. This suggests, and has been substantially well established, that while larval zebrafish detect the prey monocularly, the rest of the prey capture episode is executed using binocular vision (Bianco et al., 2011; Trivedi & Bollmann, 2013). The most interesting and intriguing feature in juvenile Medaka prey capture was that these fish never aligned themselves with the prey directly and always tended to orient themselves with the prey lateral to their body axis (Fig. 39b). As a consequence, the prey was visible only to the ipsilateral eye and never comes into the binocular field-of-view throughout the prey capture event. Furthermore, the ocular vergence angle never increases during the prey capture episode (in contrast to larval zebrafish where there is a large increase in vergence (Bianco et al., 2011).

The question now is, how do juvenile Medaka capture prey only with monocular vision? To understand this, we need to know what monocular cues the fish can successfully exploit. Our hypothesis is that juvenile Medaka rely on relative motion between the detected prey and themselves as a cue to

deciphering distance. Importantly, this explains the continuous locomotion during prey capture. Motion parallax and depth from motion are known to act as cues to assess the location and the distance to objects in a monocular context. In motion parallax, the movement of the observer results in a relative motion of objects in a scene and can serve as a powerful perceptual cue for depth perception (Wagemans, 2016; Yoonessi & Baker, 2011). A monocular observer cannot assess the distance to the object using one snap-shot of the scene. However, if now angular information is introduced along with motion the object stretches out in depth.

We observe that juvenile Medaka continuously move in a curved trajectory with respect to the prey before the final capture event. We believe this provides the fish with several angular “snap-shots” at the prey which when integrated over different time points produces a “map” which is then constantly updated with each new position and helps the fish to navigate towards the prey. Indeed, to confirm our hypothesis we computed the trajectories of the fish using all our recordings and these are shown in Fig. 40. The trajectories have been normalized so that the prey position is always at (0,0). As can be seen, all the trajectories have a curved component supporting our hypothesis that juvenile Medaka use relative motion and angular motion to resolve the position and distance to the prey.

The Medaka monocular prey capture mechanism may also explain the head snap movement. Since the hatchlings always orient themselves such that the prey is on one side of their body axis, they would have to move their head in the direction of the prey in order to consume the prey.

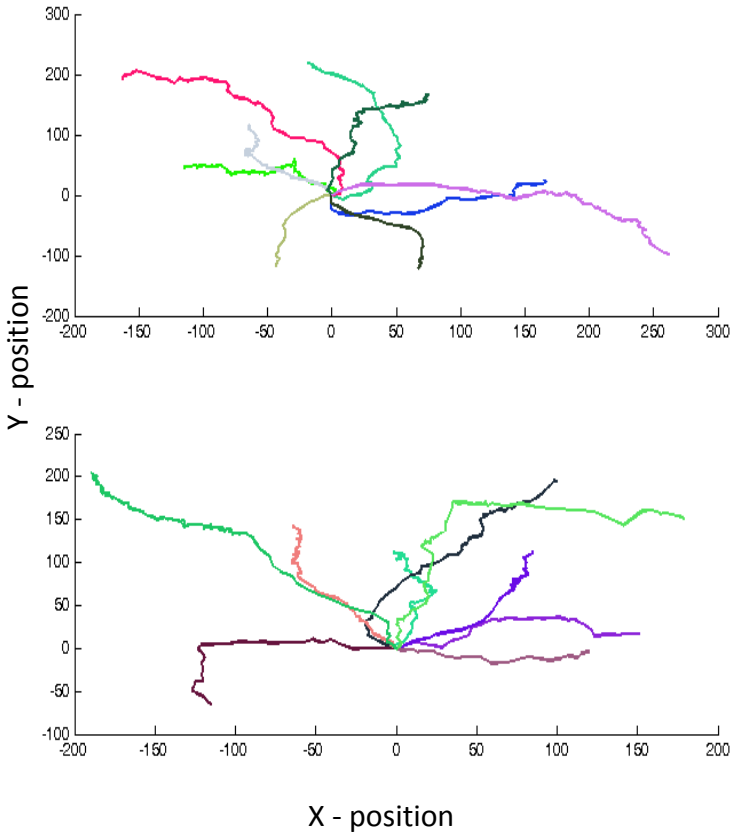

Figure 40 The trajectories during prey capture with the prey position normalized to be at (0,0) show curved paths taken by the fish to capture the prey.

In terms of evolutionary strategy, we believe juvenile Medaka use monocular vision during prey capture in order to employ the contralateral eye for detecting potential predators or competitors. Furthermore, in an environment where food is scarce, monocular vision could increase the success in foraging.

This work has shown that strategies governing an essential behavioral trait, the prey capture, may not be conserved between related species.

Outlook

It would be interesting to observe the movement of the eyes in the different strains of Medaka by minimally restraining them in a virtual environment. Such experiments can be used to study the relationship of the eye movements to the size of the prey, angular coverage of the eye and in extracting reproducible movement patterns in a more robust way.

It has been reported that sandlance fish differ from other fish optically and in the eye movements (Land, 1999b). Sandlances, similar to chameleons, avoid binocular mechanisms in prey capture and effectively capture prey with one eye. So, the focusing mechanism based on the lens-cornea combination is postulated to be the likely means to judge distances by using motion parallax. It may be useful to morphologically study the eye of the different inbred Medaka strains at high resolution to see commonalities to other organisms.

From the feeding behavior perspective, integration of morphology and behavior is the key to understanding strategies. The goal is to see how differences in morphology (for example, lip width and distance between the eyes) influence the locomotor performance and kinematics among the different strains similar to (Higham, 2007) where a relationship was shown between pectoral fin morphology and maximum gape in centrarchid fishes.

Finally, the aim is to be able to extract and quantify as many morphological and behavioral phenotypes in order that the community can benefit from this and move towards successfully establishing a genotype-phenotype map using the Medaka inbred panel.

References

Abiola, O., Angel, J. M., Avner, P., Bachmanov, A. A., Belknap, J. K., Bennett, B., . . . Complex Trait, C. (2003). The nature and identification of quantitative trait loci: a community's view. *Nat Rev Genet, 4*(11), 911-916. doi: 10.1038/nrg1206

Adams, D. C. R., F. J. and Slice, D. E. (2004). Geometric Morphometrics: Ten Years of Porgress Following the 'Revolution'. *Ital. J. Zool., 71:5-16*.

Alexander, R. M. (1967). *Functional design in fishes*. London, UK: Hutchinson University Library.

Amsterdam, A., & Hopkins, N. (2006). Mutagenesis strategies in zebrafish for identifying genes involved in development and disease. *Trends Genet, 22*(9), 473-478. doi: 10.1016/j.tig.2006.06.011

Anholt, R. R. H., & Mackay, T. F. C. (2010). *Principles of Behavioral Genetics*: Academic Press.

Atwell, S., Huang, Y. S., Vilhjalmsson, B. J., Willems, G., Horton, M., Li, Y., . . . Nordborg, M. (2010). Genome-wide association study of 107 phenotypes in Arabidopsis thaliana inbred lines. *Nature, 465*(7298), 627-631. doi: 10.1038/nature08800

Bailey, D. W. (1971). Recombinant-inbred strains. An aid to finding identity, linkage, and function of histocompatibility and other genes. *Transplantation, 11*(3), 325-327.

Bertossa, R. C. (2011). Morphology and behaviour: functional links in development and evolution. *Philos Trans R Soc Lond B Biol Sci, 366*(1574), 2056-2068. doi: 10.1098/rstb.2011.0035

Bianco, I. H., Kampff, A. R., & Engert, F. (2011). Prey capture behavior evoked by simple visual stimuli in larval zebrafish. *Front Syst Neurosci, 5*, 101. doi: 10.3389/fnsys.2011.00101

Bilder, R. M., Sabb, F. W., Cannon, T. D., London, E. D., Jentsch, J. D., Parker, D. S., . . . Freimer, N. B. (2009). Phenomics: the systematic study of phenotypes on a genome-wide scale. *Neuroscience, 164*(1), 30-42. doi: 10.1016/j.neuroscience.2009.01.027

Bloom, J. S., Ehrenreich, I. M., Loo, W. T., Lite, T. L., & Kruglyak, L. (2013). Finding the sources of missing heritability in a yeast cross. *Nature, 494*(7436), 234-237. doi: 10.1038/nature11867

Bookstein, F. L. (1998). A hundred years of morphometrics. *Acta Zoologica Academiae Scientarium Hungaricae, 44:7-59*.

Bookstein, F. L., Grayson, B., Cutting, C. B., Kim, H. C., & McCarthy, J. G. (1991). Landmarks in three dimensions: reconstruction from cephalograms versus direct observation. *Am J Orthod Dentofacial Orthop, 100*(2), 133-140. doi: 10.1016/S0889-5406(05)81520-3

Borevitz, J. O., & Nordborg, M. (2003). The impact of genomics on the study of natural variation in Arabidopsis. *Plant Physiol, 132*(2), 718-725. doi: 10.1104/pp.103.023549

Borla, M. A., Palecek, B., Budick, S., & O'Malley, D. M. (2002). Prey Capture by Larval Zebrafish: Evidence for Fine Axial Motor Control. *Brain, Behavior and Evolution, 60*(4), 207-229. doi: 10.1159/000066699

Bradski, G., & Kaehler, A. (2008). *Learning OpenCV: Computer Vision with the OpenCV Library*: O'Reilly Media.

Brady, C. A., Rennekamp, A. J., & Peterson, R. T. (2016). Chemical Screening in Zebrafish. *Methods Mol Biol, 1451*, 3-16. doi: 10.1007/978-1-4939-3771-4_1

Canny, J. (1986). A computational approach to edge detection. *IEEE Trans. Pattern Analysis and Machine Intelligence, 8*, 679 - 714.

Cheng, C. C., Peng, G. J., & Hwang, W. L. (2009). Mathworks: Pixel Connectivity. *IEEE Trans. Image Processing, 18(1): 52 - 62*.

Churchill, G. A., Airey, D. C., Allayee, H., Angel, J. M., Attie, A. D., Beatty, J., . . . Complex Trait, C. (2004). The Collaborative Cross, a community resource for the genetic analysis of complex traits. *Nat Genet, 36*(11), 1133-1137. doi: 10.1038/ng1104-1133

Cox, R. D., & Church, C. D. (2011). Mouse models and the interpretation of human GWAS in type 2 diabetes and obesity. *Dis Model Mech, 4*(2), 155-164. doi: 10.1242/dmm.000414

Driever, W., Solnica-Krezel, L., Schier, A. F., Neuhauss, S. C., Malicki, J., Stemple, D. L., . . . Boggs, C. (1996). A genetic screen for mutations affecting embryogenesis in zebrafish. *Development, 123*, 37-46.

Fero, K., Yokogawa, T., & Burgess, H. A. (2011). The Behavioral Repertoire of Larval Zebrafish. *52*, 249-291. doi: 10.1007/978-1-60761-922-2_12

Flint, J., & Mackay, T. F. (2009). Genetic architecture of quantitative traits in mice, flies, and humans. *Genome Res, 19*(5), 723-733. doi: 10.1101/gr.086660.108

Force, A., Lynch, M., Pickett, F. B., Amores, A., Yan, Y. L., & Postlethwait, J. (1999). Preservation of duplicate genes by complementary, degenerative mutations. *Genetics, 151*(4), 1531-1545.

Fu, Y., Wen, T. J., Ronin, Y. I., Chen, H. D., Guo, L., Mester, D. I., . . . Schnable, P. S. (2006). Genetic dissection of intermated recombinant inbred lines using a new genetic map of maize. *Genetics, 174*(3), 1671-1683. doi: 10.1534/genetics.106.060376

Furutani-Seiki, M., & Wittbrodt, J. (2004). Medaka and zebrafish, an evolutionary twin study. *Mech Dev, 121*(7-8), 629-637. doi: 10.1016/j.mod.2004.05.010

Gahtan, E., Tanger, P., & Baier, H. (2005). Visual prey capture in larval zebrafish is controlled by identified reticulospinal neurons downstream of the tectum. *J Neurosci, 25*(40), 9294-9303. doi: 10.1523/JNEUROSCI.2678-05.2005

Gibb, A. C., Staab, K., Moran, C., & Ferry, L. A. (2015). The Teleost Intramandibular Joint: A mechanism That Allows Fish to Obtain Prey Unavailable to Suction Feeders. *Integr Comp Biol, 55*(1), 85-96. doi: 10.1093/icb/icv042

Gonzalez, R. C., & Woods, R. E. (2002). *Digital Image Processing*: Prentice Hall.

Grisel, J. E. (2000). Quantitative trait locus analysis. *Alcohol Res Health, 24*(3), 169-174.

Herder, C., Swiercz, J. M., Muller, C., Peravali, R., Quiring, R., Offermanns, S., . . . Loosli, F. (2013). ArhGEF18 regulates RhoA-Rock2 signaling to maintain neuro-epithelial apico-basal polarity and proliferation. *Development, 140*(13), 2787-2797. doi: 10.1242/dev.096487

Higham, T. E. (2007). The integration of locomotion and prey capture in vertebrates: Morphology, behavior, and performance. *Integr Comp Biol, 47*(1), 82-95. doi: 10.1093/icb/icm021

Houle, D. (2010). Colloquium papers: Numbering the hairs on our heads: the shared challenge and promise of phenomics. *Proc Natl Acad Sci U S A, 107 Suppl 1*, 1793-1799. doi: 10.1073/pnas.0906195106

Houle, D., Govindaraju, D. R., & Omholt, S. (2010). Phenomics: the next challenge. *Nat Rev Genet, 11*(12), 855-866. doi: 10.1038/nrg2897

Hulsey, C. D., Fraser, G. J., & Streelman, J. T. (2005). Evolution and development of complex biomechanical systems: 300 million years of fish jaws. *Zebrafish, 2*(4), 243-257. doi: 10.1089/zeb.2005.2.243

Hunter, B., Wright, K. M., & Bomblies, K. (2013). Short read sequencing in studies of natural variation and adaptation. *Curr Opin Plant Biol, 16*(1), 85-91. doi: 10.1016/j.pbi.2012.10.003

Iwamatsu, T. (2004). Stages of normal development in the medaka Oryzias latipes. *Mech Dev, 121*(7-8), 605-618. doi: 10.1016/j.mod.2004.03.012

Jing, L., & Zon, L. I. (2011). Zebrafish as a model for normal and malignant hematopoiesis. *Dis Model Mech, 4*(4), 433-438. doi: 10.1242/dmm.006791

Kimura, T., Shimada, A., Sakai, N., Mitani, H., Naruse, K., Takeda, H., . . . Shinya, M. (2007). Genetic analysis of craniofacial traits in the medaka. *Genetics, 177*(4), 2379-2388. doi: 10.1534/genetics.106.068460

King, E. G., Merkes, C. M., McNeil, C. L., Hoofer, S. R., Sen, S., Broman, K. W., . . . Macdonald, S. J. (2012). Genetic dissection of a model complex trait using the Drosophila Synthetic Population Resource. *Genome Res, 22*(8), 1558-1566. doi: 10.1101/gr.134031.111

Kirchmaier, S., Naruse, K., Wittbrodt, J., & Loosli, F. (2015). The genomic and genetic toolbox of the teleost medaka (Oryzias latipes). *Genetics, 199*(4), 905-918. doi: 10.1534/genetics.114.173849

Kokel, D., & Peterson, R. T. (2011). Using the zebrafish photomotor response for psychotropic drug screening. *Methods Cell Biol, 105*, 517-524. doi: 10.1016/B978-0-12-381320-6.00022-9

Korte, A., & Farlow, A. (2013). The advantages and limitations of trait analysis with GWAS: a review. *Plant Methods, 9*, 29. doi: 10.1186/1746-4811-9-29

Kramer, D. L. a. M., R. L. (2001). The Behavioral Ecology of Intermittent Locomotion. *Amer. Zool., 41*, 137 - 153.

Land, M. F. (1992a). Visual tracking and pursuit: Humans and anthropods compared. *Journal of Insect Physiology, 38*(12), 939-951.

Land, M. F. (1992b). Visual tracking and pursuit: Humans and anthropods compared. *Journal of Insect Physiology, 38(12)*, 939-951.

Land, M. F. (1999a). Motion and vision: why animals move their eyes. *J Comp Physiol A, 185*(4), 341-352.

Land, M. F. (1999b). Visual optics: The sandlance eye breaks all the rules. *Curr Biol, 9*(8), R286-288.

Langerhans, R. B. (2008). Predictability of phenotypic differentiation across flow regimes in fishes. *Integr Comp Biol, 48*(6), 750-768. doi: 10.1093/icb/icn092

Liem, K. F. (1980). Acquisition of Energy by Teleosts: Adaptive Mechanisms and Evolutionary Patterns. *Environmenta Physiology of Fishes*, 299 - 334.

Liem, K. F., Bemis, W. E., Walker, J. W. F., & Grande, L. (2001). *Functional anatomy of the vertebrates: an evolutionary perspective*. Belmont, CA: Brooks/Cole-Thomson Learning.

Lisberger, S. G. (2010). Visual guidance of smooth-pursuit eye movements: sensation, action, and what happens in between. *Neuron, 66*(4), 477-491. doi: 10.1016/j.neuron.2010.03.027

Liti, G., Carter, D. M., Moses, A. M., Warringer, J., Parts, L., James, S. A., . . . Louis, E. J. (2009). Population genomics of domestic and wild yeasts. *Nature, 458*(7236), 337-341. doi: 10.1038/nature07743

Loosli, F., Koster, R. W., Carl, M., Kuhnlein, R., Henrich, T., Mucke, M., . . . Wittbrodt, J. (2000). A genetic screen for mutations affecting embryonic development in medaka fish (Oryzias latipes). *Mech Dev, 97*(1-2), 133-139.

Mackay, T. F., Richards, S., Stone, E. A., Barbadilla, A., Ayroles, J. F., Zhu, D., . . . Gibbs, R. A. (2012). The Drosophila melanogaster Genetic Reference Panel. *Nature, 482*(7384), 173-178. doi: 10.1038/nature10811

MacRae, C. A., & Peterson, R. T. (2015). Zebrafish as tools for drug discovery. *Nat Rev Drug Discov, 14*(10), 721-731. doi: 10.1038/nrd4627

Manolio, T. A. (2010). Genomewide association studies and assessment of the risk of disease. *N Engl J Med, 363*(2), 166-176. doi: 10.1056/NEJMra0905980

McElligott, M. B., & O'Malley D, M. (2005). Prey tracking by larval zebrafish: axial kinematics and visual control. *Brain Behav Evol, 66*(3), 177-196. doi: 10.1159/000087158

Meyer, A., & Schartl, M. (1999). Gene and genome duplications in vertebrates: the one-to-four (-to-eight in fish) rule and the evolution of novel gene functions. *Curr Opin Cell Biol, 11*(6), 699-704.

Moffatt, M. F., Traherne, J. A., Abecasis, G. R., & Cookson, W. O. (2000). Single nucleotide polymorphism and linkage disequilibrium within the TCR alpha/delta locus. *Hum Mol Genet, 9*(7), 1011-1019.

Mullins, M. C., Hammerschmidt, M., Haffter, P., & Nusslein-Volhard, C. (1994). Large-scale mutagenesis in the zebrafish: in search of genes controlling development in a vertebrate. *Curr Biol, 4*(3), 189-202.

Norton, S. F., & Brainerd, E. L. (1993). Convergence in the feeding mechanism of ecomorphologically similar species. *J. Exp. Biol., 126: 343 - 368*.

O'Malley, D. M., Zhou, Q., & Gahtan, E. (2003). Probing neural circuits in the zebrafish: a suite of optical techniques. *Methods, 30*(1), 49-63.

Pardo-Diaz, C., Salazar, C., & Jiggins, C. D. (2015). Towards the identification of the loci of adaptive evolution. *Methods Ecol Evol, 6*(4), 445-464. doi: 10.1111/2041-210X.12324

Patterson, B. W., Abraham, A. O., MacIver, M. A., & McLean, D. L. (2013). Visually guided gradation of prey capture movements in larval zebrafish. *J Exp Biol, 216*(Pt 16), 3071-3083. doi: 10.1242/jeb.087742

Peirce, J. L., Lu, L., Gu, J., Silver, L. M., & Williams, R. W. (2004). A new set of BXD recombinant inbred lines from advanced intercross populations in mice. *BMC Genet, 5*, 7. doi: 10.1186/1471-2156-5-7

Peravali, R., Gehrig, J., Giselbrecht, S., Lutjohann, D. S., Hadzhiev, Y., Muller, F., & Liebel, U. (2011). Automated feature detection and imaging for high-resolution screening of zebrafish embryos. *Biotechniques, 50*(5), 319-324. doi: 10.2144/000113669

Peterson, R. T., & Fishman, M. C. (2011). Designing zebrafish chemical screens. *Methods Cell Biol, 105*, 525-541. doi: 10.1016/B978-0-12-381320-6.00023-0

Postlethwait, J. H., Woods, I. G., Ngo-Hazelett, P., Yan, Y. L., Kelly, P. D., Chu, F., . . . Talbot, W. S. (2000). Zebrafish comparative genomics and the origins of vertebrate chromosomes. *Genome Res, 10*(12), 1890-1902.

Poynton, C. (1996). *A Technical Introduction to Digital Video*. New York: John Wiley & Sons.

Pravenec, M., Klir, P., Kren, V., Zicha, J., & Kunes, J. (1989). An analysis of spontaneous hypertension in spontaneously hypertensive rats by means of new recombinant inbred strains. *J Hypertens, 7*(3), 217-221.

Ravi, V., & Venkatesh, B. (2008). Rapidly evolving fish genomes and teleost diversity. *Curr Opin Genet Dev, 18*(6), 544-550. doi: 10.1016/j.gde.2008.11.001

Reznick, D. N., & Travis, J. (2017). Evolution: Differences can hold populations together. *Nature, 546*(7657), 218-219. doi: 10.1038/nature22502

Rohlf, F. J. a. M., L. F. (1993). A reolution in morphometrics. *Trends Ecol Evol, 8*, 129-132.

Santoriello, C., & Zon, L. I. (2012). Hooked! Modeling human disease in zebrafish. *J Clin Invest, 122*(7), 2337-2343. doi: 10.1172/JCI60434

Schall, J. D., & Thompson, K. G. (1999). Neural selection and control of visually guided eye movements. *Annu Rev Neurosci, 22*, 241-259. doi: 10.1146/annurev.neuro.22.1.241

Schartl, M. (2014). Beyond the zebrafish: diverse fish species for modeling human disease. *Dis Model Mech, 7*(2), 181-192. doi: 10.1242/dmm.012245

Sharopova, N., McMullen, M. D., Schultz, L., Schroeder, S., Sanchez-Villeda, H., Gardiner, J., . . . Coe, E. H., Jr. (2002). Development and mapping of SSR markers for maize. *Plant Mol Biol, 48*(5-6), 463-481.

Shima, A., & Mitani, H. (2004). Medaka as a research organism: past, present and future. *Mech Dev, 121*(7-8), 599-604. doi: 10.1016/j.mod.2004.03.011

Shimizu, K. K., & Purugganan, M. D. (2005). Evolutionary and ecological genomics of Arabidopsis. *Plant Physiol, 138*(2), 578-584. doi: 10.1104/pp.105.061655

Sinn, R., Peravali, R., Heermann, S., & Wittbrodt, J. (2014). Differential responsiveness of distinct retinal domains to Atoh7. *Mech Dev, 133*, 218-229. doi: 10.1016/j.mod.2014.08.002

Slatkin, M. (2008). Linkage disequilibrium--understanding the evolutionary past and mapping the medical future. *Nat Rev Genet, 9*(6), 477-485. doi: 10.1038/nrg2361

Soule, M. (1967). Phenetics of Natural Populations I. Phenetic Relationships of Insular Populations of the Side-Blotched Lizard. *Evolution, 21*(3), 584-591. doi: 10.1111/j.1558-5646.1967.tb03413.x

Spivakov, M., Auer, T. O., Peravali, R., Dunham, I., Dolle, D., Fujiyama, A., . . . Wittbrodt, J. (2014). Genomic and phenotypic characterization of a wild medaka population: towards the establishment of an isogenic population genetic resource in fish. *G3 (Bethesda), 4*(3), 433-445. doi: 10.1534/g3.113.008722

Stinchcombe, J. R., & Hoekstra, H. E. (2008). Combining population genomics and quantitative genetics: finding the genes underlying ecologically important traits. *Heredity (Edinb), 100*(2), 158-170. doi: 10.1038/sj.hdy.6800937

Takeda, H., & Shimada, A. (2010). The art of medaka genetics and genomics: what makes them so unique? *Annu Rev Genet, 44*, 217-241. doi: 10.1146/annurev-genet-051710-151001

Trivedi, C. A., & Bollmann, J. H. (2013). Visually driven chaining of elementary swim patterns into a goal-directed motor sequence: a virtual reality study of zebrafish prey capture. *Front Neural Circuits, 7*, 86. doi: 10.3389/fncir.2013.00086

Vincent, L. (1993). Grayscale area openings and closings, their efficient implementation and applications. *Proc. EURASIP Workshop on Mathematical Morphology and its Applications to Signal Processing*, 22 - 27.

Wagemans, J. E. (2016). *The Oxford Handbook of Perceptual Organization*.

Wainwright, P. C. (1999). Ecomorphology of Prey Capture in Fishes. *Ichthyology*, 403 - 415.

Westerfield, M. (2007). *The Zebrafish Book: A Guide for the Laboratory Use of Zebrafish (Danio Rerio)*: Eugene,, OR: University of Oregon Press.

Wittbrodt, J., Shima, A., & Schartl, M. (2002). Medaka--a model organism from the far East. *Nat Rev Genet, 3*(1), 53-64. doi: 10.1038/nrg704

Yamamoto, T. O. (1953). Artificially induced sex-reversal in gentoypic males of the medaka (Oryzias Latipes). *J Exp Zool, 123: 571 - 594*.

Yoonessi, A., & Baker, C. L., Jr. (2011). Contribution of motion parallax to segmentation and depth perception. *J Vis, 11*(9), 13. doi: 10.1167/11.9.13

Zeng, W., Gao, W., & Zhao, D. (2003). Automatic moving object extraction in MPEG video. *Proceedings of the 2003 International Symposium on Circuits and Systems*.

Zon, L. I., & Peterson, R. T. (2005). In vivo drug discovery in the zebrafish. *Nat Rev Drug Discov, 4*(1), 35-44. doi: 10.1038/nrd1606